Brigham Young University
BYU ScholarsArchive

Theses and Dissertations

2023-08-15

Improved Endmember Mixing Analysis (EMMA): Application to a Nested Catchment, Provo River, Northern Utah

Alyssa Nicole Thompson
Brigham Young University

Follow this and additional works at: https://scholarsarchive.byu.edu/etd

 Part of the Physical Sciences and Mathematics Commons

BYU ScholarsArchive Citation

Thompson, Alyssa Nicole, "Improved Endmember Mixing Analysis (EMMA): Application to a Nested Catchment, Provo River, Northern Utah" (2023). *Theses and Dissertations*. 10218.
https://scholarsarchive.byu.edu/etd/10218

This Thesis is brought to you for free and open access by BYU ScholarsArchive. It has been accepted for inclusion in Theses and Dissertations by an authorized administrator of BYU ScholarsArchive. For more information, please contact ellen_amatangelo@byu.edu.

Improved Endmember Mixing Analysis (EMMA): Application to a Nested Catchment, Provo River, Northern Utah

Alyssa Nicole Thompson

A thesis submitted to the faculty of
Brigham Young University
in partial fulfillment of the requirements for the degree of

Master of Science

Gregory T. Carling, Chair
Barry R. Bickmore
Stephen T. Nelson
Joshua J. LeMonte
Zachary Aanderud

Department of Geological Sciences

Brigham Young University

Copyright © 2023 Alyssa Nicole Thompson

All Rights Reserved

ABSTRACT

Improved Endmember Mixing Analysis (EMMA): Application to a Nested Catchment, Provo River, Northern Utah

Alyssa Nicole Thompson
Department of Geological Sciences, BYU
Master of Science

An endmember mixing analysis (EMMA) is a hydrograph separation technique used to identify and quantify stream source contributions, but the error within the results of the analysis itself can be difficult to quantify. Employing EMMA to accurately quantify these contributions is particularly important for critical watersheds that supply water to large populations, such as montane watersheds. We applied EMMA to the Provo River, a nested catchment with three monitoring locations in northern Utah, to understand the limitations and potential improvements that could be made to EMMA. Four main endmembers (quartzite groundwater, soil water, snow and carbonate groundwater) were identified for the watershed and differentiated using the conservative tracers $\delta^{18}O$, $\delta^{2}H$, Si, HCO_3^-, Mg^{2+}, K^+, and Ca^{2+}. In a traditional EMMA approach, a principal components analysis (PCA) is used to identify endmembers for a single location in a watershed, and the principal component (PC) scores are used to calculate the fractional contributions of each endmember. However, we found that calculating the fractional contributions of the endmembers in tracer space resulted in less error in the calculations compared to performing the calculation in PC defined space (U-space). Performing the mixing in tracer space with four endmembers showed that during spring runoff, snow was the main endmember with inputs ranging from 23 – 66% for the highest part of the watershed and 14 – 60% for the lowest part of the watershed. During baseflow, the stream was dominated by groundwater with contributions ranging from 23 – 60% quartzite groundwater for the upper part of the watershed and 30 – 57% carbonate groundwater for the lower part of the watershed. The amount of error present in the results depended on the scale of the catchment and the number of endmembers included, with more error in downstream locations relative to upstream locations. The nested catchment approach is a further improvement on traditional EMMA because it allows for identification of missing endmembers and error analysis for characterizing stream chemistry in several locations in a complex watershed.

Keywords: EMMA, endmember mixing analysis, PCA, Provo River, catchment hydrology, nested catchment

ACKNOWLEDGEMENTS

I would like to thank Dr. Greg Carling for encouraging me to apply to graduate school and for helping me to develop such important field, lab, and writing skills. I would like to especially thank Dr. Barry Bickmore for the extensive amount of time spent meeting to discuss the complex math and statistics in my thesis and encouraging me to be a better researcher. Thank you to the rest of my committee for giving me valuable feedback and supporting my ideas. I would like to thank Kevin Rey for helping me process the many samples I had in the lab and his patience as I learned how to use the different instruments. I am grateful to all of the students who helped to collect river samples over the years, particularly Kendra Caskey, Hannah Wehrmeister, and Miaja Coombs. Lastly, I would like to thank my incredible husband Carson for supporting me throughout my education.

TABLE OF CONTENTS

LIST OF TABLES

LIST OF FIGURES

1. Introduction

Quantifying water sources to alpine streams is critical for managing water resources in mountain watersheds. At least one sixth of the world's population rely on snowpack melt from mountain watersheds, but climate and water use changes threaten this critical resource (Barnett et al., 2005). High alpine streams contain a mixture of both surface and subsurface sources, the contributions of which vary widely between snowmelt runoff and baseflow (Foks et al., 2018). Hydrograph separation methods, including endmember mixing analysis (Christopherson et al., 1990), are used to quantify water source contributions in relatively complex watersheds. Common water sources (endmembers) in high alpine watersheds include groundwater, precipitation, snow, and soil water (Christopherson & Hooper, 1992). The endmembers are defined by chemical or isotopic tracers that permit differentiating the water body of interest by each source (Christopherson et al., 1990; Hooper, 2003). Common tracers include Ca^{2+}, Mg^{2+}, K^{+}, Na^{+}, Fe, Si, Cl^{-}, HCO_3^{-}, NO_3^{-}, $\delta^{18}O$, $\delta^{2}H$, and electrical conductivity, depending on whether the tracer behaves conservatively or not (Barthold et al., 2011). Characterizing stream flows in terms of these sources may be used to better understand the chemical evolution and changes in water sources to a stream over time.

An endmember mixing analysis (EMMA) is useful for estimating endmember contributions to streams, including complex watersheds. EMMA uses a principal components analysis (PCA) to reduce the dimensionality of the data, making it easier to visualize and identify clusters of elemental numeric data (Christopherson & Hooper, 1992). Visualizing the data in terms of dimensionally reduced space allows for identifying the potential endmembers that circumscribe the stream data. The extent of mixing between the various endmembers is calculated by solving a system of linear equations to obtain the fractional contributions of each

endmember, with the mixing calculation primarily being done using the data in terms of the dimensionally reduced space (Christopherson & Hooper, 1992).

The ability of EMMA models to accurately represent hydrological reality depends on two main factors. First, the computational method used in the mixing calculations can affect the degree to which the fractional contributions of the endmembers are optimized. Many studies calculate the mixing in the dimensionally reduced space (Foks et al., 2018; Lukens et al., 2022; Wilson et al., 2016), but this approach is more prone to error in the calculation of the fractional contributions**.** Second, abstracting a real-world stream as a simple mixture of a few endmembers will always be an oversimplification, and the degree to which that is the case exerts a limitation on model accuracy that can be difficult to quantify. Some methods exist for determining the extent of error within the endmember datasets, such as gaussian error propagation, bootstrapping, or Monte Carlo simulations (Bazemore et al., 1994; Christopherson et al., 1990; Genereux, 1998; Vonk et al., 2010; Xu Fei & Harman, 2022). However, EMMA can produce plausible results that may be qualitatively inaccurate, and more information is needed to estimate how accurately the endmembers define the stream chemistry.

The purpose of our study is to critically evaluate existing EMMA approaches and provide recommendations to yield more reliable results. The primary objectives are to: (1) develop an alternative approach to EMMA to minimize error in the mixing calculation and allow for a more complex analysis by including more endmembers; and (2) use a nested-catchment approach to narrow down the location of missing endmembers and tease out inaccuracies in the model that are difficult to identify via a traditional error analysis.

Our study focuses on three monitoring sites in the upper Provo River, a snow-dominated perennial stream located in the Uinta Mountains of northern Utah. The Provo River is part of the

drinking water supply for over half of Utah's population. The upper Provo River watershed is an ideal field area with abrupt transitions in underlying lithology, allowing for a nested catchment study with monitoring locations within each rock type. Most EMMA studies are applied to a small watershed with a single monitoring location to characterize changes in endmember inputs over time (Barthold et al., 2010; Cuoco et al., 2021; Durand & Torres, 1996; Guinn et al., 2010). We show that applying EMMA to multiple monitoring locations along an alpine stream in a nested catchment allows for better endmember identification and mixing error analysis by quantifying inputs between locations.

2. Methods

An endmember mixing analysis (EMMA) is a tracer-based hydrograph separation technique that is carried out via the following steps as described in Christopherson and Hooper (1992) and Christopherson et al. (1990): (1) measure chemistry of the water to be analyzed (e.g., stream water) and water sources that could be used as potential endmembers for the hydrograph separation (e.g., groundwaters, precipitation, soil water, etc.); (2) determine which solutes or isotopes appear to behave conservatively, and so could be used as tracers; (3) identify which potential endmembers can be plausibly applied to the model using a principal components analysis; (4) optimize the mixing models to calculate the fractional contributions from the selected endmembers to the resulting mixture; and (5) perform an error analysis of the endmember datasets. In the following subsections, we describe the sites where we applied EMMA and provide further details of how we have modified established EMMA methods to improve mixing estimates.

2.1 Upper Provo River watershed site description

The upper Provo River watershed covers 675 km^2 in the southwestern Uinta Mountains of northern Utah (Figure 1). The watershed is dominantly fed by high elevation snowmelt and receives diverted water from the Duchesne River and Weber River as part of the Provo River Project (U.S. Bureau of Reclamation, 1958). The upper Provo River extends ~50 km with a vertical relief of 1000 m, from 2900 m asl at the headwaters at Trial Lake to 1900 m asl at Jordanelle Reservoir. Three monitoring stations are located, from upstream to downstream, at Soapstone, Woodland, and Hailstone, with the rate of discharge generally increasing from Soapstone to Hailstone (Figure 2).

The geology of the upper part of the watershed contains mainly silica-cemented sandstone with minor amounts of shale overlain by glacial and other Quaternary deposits (Figure 1). The depth of the soil in the upper area of the watershed is typically ~1 m (Munroe et al., 2015), enriched by dust in the A soil horizons (Munroe et al., 2020). The lower part of the watershed contains primarily Paleozoic sedimentary rocks between Soapstone and Hailstone with Tertiary volcanic rocks between Woodland and Hailstone. The upper part of the watershed is mostly undeveloped except for the Mirror Lake Highway and several campgrounds. The lower part of the watershed is more developed with agricultural fields, small towns, and maintained roads.

2.2 Stream and endmember water sample collection

Stream samples included in the study were collected along Provo River from the 2016 to 2018 water years, and again for the 2021 and 2022 water years. Sampling occurred biweekly to monthly except for the months following the snowmelt runoff period, where sampling occurred

once or twice weekly (April – June). A total of 318 stream samples were collected during these collection periods, with 106 collected from Soapstone, 106 from Woodland, and 106 from Hailstone (Table 1). Potential endmember samples for were collected between 2012 and 2022 (Table 4). Stream and endmember samples included separate subsamples for major cations and trace elements, major anions, bicarbonate, and $\delta^{18}O$ and $\delta^{2}H$ isotopes. Samples for major cations and trace elements were filtered with a 0.45 μm PES syringe filter into an acid-washed 60 mL LDPE bottle and acidified to 2.4% v/v TMG nitric acid. Samples for major anions and bicarbonate were collected in a 1 L plastic bottle and further processed in the lab. Water samples for $\delta^{18}O$ and $\delta^{2}H$ analysis were collected in amber glass bottles with Polyseal caps to prevent evaporation. All samples were refrigerated until analysis.

Snowpack endmember samples (n = 22) were collected prior to spring snowmelt at maximum accumulation. Samples were collected by digging snow pits and taking a cross section of snow using an acid-washed plastic tube. Sample from the plastic tube was deposited into FLPE acid-washed bottles. The bottles were taken into the lab and melted, then sub-sampled for chemical analysis.

Soil water endmember samples (n = 6) were collected during spring snowmelt to allow for maximum saturation of the soils. Sample was collected by using a small shovel to collect both soil and water, placed into a plastic bag, and refrigerated. Saturated soils were transferred into 50 mL centrifuged tubes and centrifuged at 6000 rpm for 20 minutes. Sample was decanted and sub-sampled for various analyses.

Quartzite (n = 9) and carbonate (n = 8) groundwater endmember samples were collected from springs throughout the watershed during baseflow but before snowfall (between July and October). Samples were collected at this time to get a representative value for isotopic ratios with

limited mixing with snow or ice. Springs discharging from quartzite and carbonate are classified as quartzite and carbonate groundwater, respectively. Although no carbonate or quartzite groundwater springs were sampled in the Weber or Duchesne watershed, the chemistry of these endmembers was assumed to be uniform across the three watersheds.

2.3 Laboratory analysis

Stream and endmember samples were analyzed using similar methods. Major cations and trace elements were analyzed using an Agilent 7500ce quadrupole inductively coupled plasma mass spectrometer (ICP-MS). The following elements were measured for all stream and endmember samples: Al, As, B, Ba, Be, Ca, Cd, Ce, Co, Cr, Cs, Cu, Dy, Er, Eu, Fe, Gd, Ho, K, La, Li, Lu, Mg, Mn, Mo, Na, Nd, Ni, Pb, Pr, Rb, Sb, Sc, Se, Sm, Sr, Tb, Th, Tl, U, V, Y, Yb, and Zn. Further descriptions of the methods are given in Checketts et al. (2020). Inductively coupled plasma optical emissions spectroscopy (ICP-OES) was additionally used to analyze for Si as the detection limits through ICP-MS were insufficient to accurately determine Si concentrations. Major anion (F^-, Cl^-, NO_3-, and SO_4^{2-}) concentrations were analyzed using a Dionex ICS-90 chromatograph (IC). HCO_3^- concentrations were analyzed through an alkalinity test on unfiltered samples by acid titration using a Mettler Toledo DL50 titrator on the samples collected before 2020, and titrated by hand using a Hach alkalinity test kit on the samples collected after 2020. Alkalinity values were assumed to be equal to bicarbonate concentrations. Stable isotope ($\delta^{18}O$ and δ^2H) ratios in water were analyzed using a Los Gatos Research Liquid Water Isotope Analyzer. All samples are reported relative to Vienna Standard Mean Ocean Water (VSMOW).

2.4 Data quality control

Where solute concentrations are low, small changes in solutes greatly influence the charge balance. To set the charge balance, any sample that was outside of +/- 5% charge balance error was adjusted by varying the bicarbonate concentration. Bicarbonate values were determined to be the solute concentrations with the most uncertainty and were adjusted in 50 out of 106 Soapstone samples, 22 out of 106 Woodland samples, and 17 out of 106 Hailstone samples. The average adjustments for Soapstone, Woodland, and Hailstone were 9.5 mg/L, 13.5 mg/L and 24.5 mg/L, respectively. Of the total adjustments made, 88% of the samples were adjusted from samples collected during 2020 and later. This is likely due to the change in methods in measuring alkalinity beginning in 2020. The adjustments result in values that were linearly consistent with the samples collected from the three previous water years when plotted against other solutes.

2.5 Tracer selection

To evaluate which tracers could be used in the mixing analysis, we estimated the potential conservative behavior of isotopes and solutes in the full dataset. Isotopes and solute concentrations are considered conservative if they do not undergo isotopic fractionation or participate in chemical reactions, which can be observed by linear relationships in bivariate plots (Christopherson & Hooper, 1992). The set of solutes or isotopes to include as tracers must exhibit linear behavior with respect to each other. $\delta^{18}O$ and $\delta^{2}H$ values can be assumed to be conservative, even if they do not exhibit linear relationships with respect to the solute tracers. This is because $\delta^{18}O$ and $\delta^{2}H$ track elevation and meteoric precipitation (Clark & Fritz, 1997) and therefore variations arise from fundamentally different process than for the solute tracers.

We used a step-wise approach to determine the best conservative tracers to include in the analysis. The conservative behavior of potential tracers was determined from an array of 49 elements and two stable isotopes, $\delta^{18}O$ and $\delta^{2}H$. As many conservative elements as possible were retained to maximally constrain the mixing models. In our case, bivariate plots of solutes and isotopes with strong linear relationships ($R > 0.80$) were determined to behave conservatively. A key principle of an endmember mixing analysis is for the endmembers to have distinct chemical or isotopic composition (Cuoco et al., 2021; James & Roulet, 2006). By including all conservative solutes or isotopes in the analysis, tracers representing each endmember are more likely to be recognized.

2.6 Data formatting and standardization

In preparation for applying EMMA, both the stream and endmember data must be properly organized and standardized. Let **R** be an $m \times n$ matrix where m is the number of stream water samples and n is the number of tracers. We will refer to each column of **R** as vector $\vec{r}_j$, which is the collection of tracer *j* values in the m stream water samples. The individual elements of matrix **R**, r_{ij}, are the concentrations (or isotopic ratios) of tracer *j* in sample *i*. Prior to the PCA, concentrations in the matrix **R** were standardized using z-scoring, where the mean of each column of the solute data is subtracted from the values in the column, and then divided by the standard deviation of that column. This allows each column to have a mean of zero and a standard deviation of 1, ensuring that the subsequent analysis is not dominated by variables with large absolute values (Christopherson & Hooper, 1992). The resulting matrix, $\mathbf{R}_z$, is then composed of column vectors $\vec{r}_{z_{ij}}$, which are the z-scored values of tracer *j* in sample *i*.

$$\mathbf{R} = [\vec{r}_1 \quad \dots \quad \vec{r}_j \quad \dots \quad \vec{r}_n] = \begin{bmatrix} r_{11} & \dots & r_{1j} & \dots & r_{1n} \\ \vdots & \ddots & \vdots & \ddots & \vdots \\ r_{i1} & \dots & r_{ij} & \dots & r_{in} \\ \vdots & \ddots & \vdots & \ddots & \vdots \\ r_{m1} & \dots & r_{mj} & \dots & r_{mn} \end{bmatrix} \tag{1}$$

$$r_{z_{ij}} = \frac{r_{ij} - \mu_{\vec{r}_j}}{\sigma_{\vec{r}_j}} \tag{2}$$

Prior to applying EMMA, each dataset of individual endmembers should be averaged together to create a single sample that represents the single endmember for that area. Each of these averaged endmembers should then be arranged in a *d*×*n* matrix (**M**), where *d* is the number of averaged potential endmembers and *n* is the number of tracers. Prior to calculating the principal component (PC) scores for the endmembers, concentrations are first standardized using the mean and standard deviation of the stream sample tracers. The new matrix of standardized endmember values is $\mathbf{M}_z$.

$$\mathbf{M} = [\vec{m}_1 \quad \dots \quad \vec{m}_j \quad \dots \quad \vec{m}_n] = \begin{bmatrix} m_{11} & \dots & m_{1j} & \dots & m_{1n} \\ \vdots & \ddots & \vdots & \ddots & \vdots \\ m_{i1} & \dots & m_{ij} & \dots & m_{in} \\ \vdots & \ddots & \vdots & \ddots & \vdots \\ m_{d1} & \dots & m_{dj} & \dots & m_{dn} \end{bmatrix} \tag{3}$$

$$m_{z_{ij}} = \frac{m_{ij} - \mu_{\vec{r}_j}}{\sigma_{\vec{r}_j}} \tag{4}$$

2.7 Principal components analysis

A principal components analysis (PCA) is performed on the standardized stream data $\mathbf{R}_z$ to determine which potential endmembers to use in EMMA. A PCA is a dimensional reduction technique used to reduce the number of variables to a more manageable level. In a PCA, a new

set of n variables (principal components or PCs), composed of linear combinations of the n original variables, is created by rotating the original axes to maximize the amount of data variance explained by the fewest number of PCs. The PCs are then ranked in descending order of how much data variance they describe, so that the first principal component (PC_1) describes the most variance and PC_n describes the least. The PCs contain the same information as the original data, but if some of the later PCs are discarded, less information is lost than if the same number of the original variables were discarded.

In our case, this was done using the MATLAB® *pca* function, which accepts $\mathbf{R}_z$ as input and produces several outputs, including the following. First, it produces an $n \times n$ coefficient matrix, $\mathbf{C_R}$, composed of column vectors representing the coefficients of linear equations that transform the original data coordinates into principal component space (Table 2). A matrix of principal component scores ($\mathbf{R}_{PC}$), contains the original data values transformed in terms of the new principal components in rotated data space, and is produced by multiplying the matrix $\mathbf{R}_z$ by $\mathbf{C_R}$.

$$\mathbf{R}_{PC} = \mathbf{R}_z * \mathbf{C_R} \tag{5}$$

Next, the function produces an $n \times 1$ vector ($\vec{e}_{\mathbf{R_{PC}}}$) of eigenvalues of the covariance matrix of $\mathbf{R}_z$, where each value represents the amount of variance explained by the corresponding principal component. An eigenvalue of one (for z-scored data) would mean that the corresponding principal component explains the same amount of variance as any one of the original variables, whereas any value higher than one would mean that it explains more variance than the original variables (Davis, 2002). The principal components are arranged in descending order of the amount of variance they explain, so one retains the first few principal components and discards

the rest to reduce the dimensionality of the data while retaining as much of the total variance as possible.

There are multiple ways to determine the number of principal components to retain for the analysis. For example, the rule of one involves retention of all PCs with eigenvalues equal to or greater than 1 (Barthold et al., 2010; James & Roulet, 2006; Joreskog et al., 1976), meaning that they explain at least as much variance as the original variables. Perhaps a more practical approach is to analyze residual plots by back-calculating stream water concentrations using different numbers of retained PCs and subtracting the original stream water concentrations to observe whether the residuals exhibit any structure (Hooper, 2003). The number of PCs to retain is indicated by iteratively increasing the number of PCs and stopping when there is no observed structure in the residual plots. This ensures that enough information is retained to adequately represent all tracers. Another method includes creating a scree plot which is especially useful if the user intends for the model to explain a certain percent of the total variance in their analysis. A scree plot typically shows a steep decline in the magnitude of eigenvalues as the number of PCs increase, with the plot eventually flattening out beyond a certain point. This point is known as the "elbow" of the plot, and its location indicates the number of PCs to retain in the analysis (Cattell, 1966).

2.8 Endmember selection

Once a subset of the PCs is retained for further use, the space defined by these PCs is called U-space (Christopherson & Hooper, 1992) and the data are projected on U-space for visual examination to aid in endmember selection. The minimum number of endmembers to include in the analysis is the number of retained PCs plus one (Christopherson & Hooper, 1992).

That is, it takes at least three points to circumscribe a cloud of data in two-dimensional space, and four points to circumscribe a cloud of data in three-dimensional space. If more than three PCs are retained, selecting the appropriate number of endmembers becomes more challenging as only three-dimensions can be visually represented at once (Davis, 2002). Because U-space must be defined by the stream data and not the endmember data, PC scores for the stream endmembers are calculated using the coefficient matrix $\mathbf{C_R}$. The PC scores for the endmembers are calculated from the standardized endmember values $\mathbf{M}_z$ and multiplied by the coefficient matrix $\mathbf{C_R}$.

$$\mathbf{M}_{PC} = \mathbf{M}_z * \mathbf{C_R} \quad (6)$$

The selected PC scores for the stream water and endmembers samples are then projected into U-space to determine which set of endmembers adequately circumscribe the data. The selected endmembers are then treated as the main sources of water for the watershed. From this point forward, $\mathbf{M}_z$ will be constructed from the standardized mean tracer values of only the selected endmembers. The primary purpose of the PCA is to select endmembers for the analysis, and we propose that the mixing calculation should be performed in the original tracer space rather than in U-space, as described below.

2.9 Mixing calculation

The primary purpose of the PCA is to select plausible endmembers for the mixing analysis, but past studies have gone further by performing the mixing calculations in U-space (defined by the subset of retained PCs). We argue that there is no compelling reason to adopt this strategy, and that performing the mixing calculations in standardized tracer space is preferable.

Mixing models are most commonly used to determine the fractional input from multiple sources (endmembers) to the main area of interest, like a stream or sediment sample. A general

way of expressing this mixing is in the form of a summation (Albarède, 2009), where C_0^j is the concentration of tracer *j* in the stream sample, f_d is the fractional contribution from endmember *d*, and C_d^j is the concentration of tracer *j* in endmember *d* and *w* is the collection of endmembers within *d*. This solution adheres to the principle of conservation of mass by assuming that the concentrations of all defined inputs or endmembers into the system will fully explain the concentrations in the mixture. This introduces the following set of constraints:

$$\sum_{w=1}^{d} f_w = 1 \tag{7}$$

$$C_0^j = \sum_{w} f_w C_w^j \tag{8}$$

The summations may then be solved for the f_d values as a system of linear equations. This can be done via direct calculation (e.g., Gaussian elimination, etc.) if the system is critically determined (i.e., the number of variables equals the number of equations), but this does not allow one to constrain the f_d values to be non-negative, which can lead to non-physical results (Ali et al., 2010; Liu et al., 2004). Therefore, it is preferable to solve the system via optimization, which can deal with both critically determined and overdetermined (the number of variables is less than the number of equations) systems and can include various types of constraints. This defines the system of equations as a constrained, least-squares linear estimation problem to solve for the fractional contributions of each source as described in Christophersen (1990), where *n* is the number of *j* tracers in the dataset. In any case, where $n > (d - 1)$, the system results in an overdetermined system of equations.

$$1 = f_1 + f_2 + \ldots f_d$$

$$C_0^j = f_1 C_1^j + f_2 C_2^j + \cdots f_d C_d^j \quad (9)$$

$$C_0^n = f_1 C_1^n + f_2 C_2^n + \cdots f_d C_d^n$$

These linear equations have been traditionally solved using the concentrations defined by tracer space, where endmembers would typically be selected by determining which endmembers best circumscribed the data in each bivariate plot of the tracers used in the analysis.

Rather than using the raw or standardized tracer concentrations in the system of linear equations, Christopherson and Hooper (1992) recommended using the composite concentrations in the retained PC scores of the stream and endmember samples as the input (c.f., Barthold et al., 2010; Christopherson et al., 1990). (Each PC depends on all of the original variables to different degrees, which is why we refer to them as composite variables.) However, using the retained PC scores for the mixing calculation can generally lead to inaccuracy in the results because the scores represent only a fraction of the total information contained in the raw or standardized data. Using the PC scores for the mixing calculation is an unnecessary step, and instead, the full set of standardized data should be used. To address this in our study, fractional contributions were calculated both using standardized stream water data and the PC scores for the stream data and compared using the optimization described in Christopherson et al. (1990).

We set up the optimization as shown in Equations 10 – 11. The objective function minimized in our analysis is the sum of squared error, where the inputs include an $n \times d$ matrix of standardized endmember values ($\mathbf{M}_z$) and an $n \times 1$ column vector of standardized stream water concentrations from each row in matrix $\mathbf{R}_z$. The constraints on the optimization include that the sum of the fractional contributions should be equal to 1, and the value of each contribution can only be between 0 and 1. This calculation is then used for each stream sample to determine the fractional contribution of each endmember for a given sampling day.

$$E_j = \left(\mathbf{M_Z} * \vec{f}\right) - \vec{\mathbf{r}}_{\mathbf{z_j}} \tag{10}$$

$$\underset{x\in[0,1]}{\arg\min}\left(\sum_{j=1}^{n} {E_j}^2\right), \qquad \text{subject to: } \sum_{w=1}^{d} f_w = 1 \tag{11}$$

In our case, the fractional contribution values in $\vec{f}$ were optimized for each stream sample using the MATLAB function *fmincon*. This function minimizes an objective function to determine the best values for the adjustable parameters, given a set of initial guesses and various types of constraints. Initial guesses for each endmember were set to *1/d,* where *d* is the number of endmembers used in the analysis. The output from *fmincon* is a *d×1* column vector ($\vec{f}$) of estimated fractional contributions for a single stream sample, where the elements (f_w) are the individual endmember contributions in the order they were arranged in $\mathbf{M}_z$.

$$\vec{f} = \begin{pmatrix} f_1 \\ f_2 \\ \vdots \\ f_d \end{pmatrix} \tag{12}$$

The fractional contributions calculated for each sampling day were plotted in a stacked bar graph to observe how these contributions changed over time. A weighted discharge plot can also be created by multiplying the fractional contributions by the rate of discharge measured at the time of sample collection to observe seasonal fluctuations of the relative contributions from each endmember.

2.10 Residual analysis

To check the accuracy of the model and the endmembers selected, the predicted concentrations based on the estimated fractional contributions are compared to the actual stream chemistry for each sampling day (Foks et al., 2018). To convert the estimated fractional contributions into stream concentrations, the vector $\vec{f}$ is multiplied by the matrix of standardized endmembers, resulting in a *m*×*n* matrix of predicted standardized stream values, $\mathbf{R}_{\mathbf{z}}^{*}$. Each standardized value is then de-standardized using the standard deviation and mean calculated for each tracer from the original matrix **R**.

$$\mathbf{R}_{\mathbf{z}}^{*} = \mathbf{M}_{\mathbf{z}} * \vec{x} \tag{13}$$

$$\boldsymbol{r}_{\mathbf{z}}^{*} = \left(r_{z_{ij}}^{*} * \sigma_{\mathbf{r}_j}\right) + \mu_{\mathbf{r}_j} \tag{14}$$

The predicted concentrations are then plotted against the observed concentrations and assessed for linearity and adherence to the 1:1 line. Those tracers which are under- or overpredicted by the model indicate the possible need for an additional endmember, or suggests a chemical process which makes them non-conservative.

2.11 Endmember error analysis

An error analysis was performed on the endmembers using jackknifed mean values of the endmember tracer compositions to measure the error due to the variations in the endmember samples collected. This method was used on the original endmember datasets before they were averaged together. The method of jackknifing the mean includes generating a distribution of mean values by systematically excluding a single observation and averaging the remaining observations (Trauth, 2021). This error method is used to account for the existing error within the endmember samples. As mentioned above, the endmembers used in the model are each

composed of a group of samples that are averaged together to represent the endmember. If each group of samples for an individual endmember had *m* samples, then a new representative averaged endmember would be created by removing one sample from the dataset and averaging the remaining *m*-1 samples together. This would be repeated *m* times, creating a new matrix the same dimensions as the initial matrix of endmember samples, but now containing a variety of averaged endmember values for the individual endmember. This is repeated for each endmember used in the analysis, and the averaged groups calculated for each endmember are then arranged in every possible combination and used in the optimization for every sample collected. If a dataset then had four endmembers and 10 samples collected for each endmember, there would be 10,000 iterations of different averaged endmember combinations used to calculate the fractional contribution of each endmember for each sample in the dataset. The resulting mean and standard deviation for the percent contribution between all of the iterations for each sampling day are then used to quantify the extent of error due to endmember sampling. The MATLAB function *jackknife* was used to calculate the jackknifed mean values for each endmember.

2.12 Calculation of model misfit for non-tracers

It may sometimes be possible to infer processes contributing to non-conservative behavior by examining how solutes other than the original tracers are underpredicted or over predicted by the model. The magnitude of the misfit can be calculated by fitting an equation (not necessarily linear) to the residuals of the predicted and observed solute values, then subtracting the real solute concentrations from those predicted by the equation.

3. Results

3.1 Conservative tracer selection

From the bivariate plots (Figure 3) we selected $\delta^{18}O$, $\delta^{2}H$, Si, HCO_3^-, Mg^{2+}, K^+, and Ca^{2+} as conservative tracers, because the correlation between the solutes was $R > 0.80$. Na^+ and Cl^- were highly correlated with each other but were determined to be poorly suited for the model since their R values relative to other conservative solutes were < 0.80. Although Na^+ and Cl^- likely behave conservatively in the watershed, they were not used in the model because of relatively poor linear correlations in bivariate plots driven by unexplained sources of enrichment in the lower part of the watershed, as discussed below.

3.2 Endmember selection for the Provo River watershed

The minimum number of endmembers to include in the analysis depends on how many PCs are required to explain a reasonable amount of variance in the dataset. The number of principal components to include was determined by applying the "rule of one", a scree test, and assessing the residual structure in the stream values for each tracer. Only the first and second PCs had eigenvalues greater than one, suggesting a three-endmember model to describe the stream data according to the rule of one. The scree test (Figure 4) and the structure in the residuals (Figure 5) additionally validated the use of two PCs to describe the data.

In our case, the endmembers that best circumscribed the data in two-dimensional U-space were quartzite groundwater, snow, and carbonate groundwater. However, a previous study showed that soil water has a strong influence on Provo River chemistry during spring runoff (Checketts et al., 2020). Therefore, a third PC was included because there was an *a priori* reason for including a fourth endmember. The first three PCs explain 95.4% of the variance in the

original, z-scored stream dataset. The arrangement of the endmembers around the stream data in U-space was assessed in combined plots of PC1, PC2, and PC3 scores (Figure 6).

3.3 Model predicted concentrations versus observed concentrations for selected tracers

The model predicted concentrations of $\delta^{18}O$, $\delta^{2}H$, Si, HCO_3^-, Mg^{2+}, K^+, and Ca^{2+} were compared to the observed stream data to assess the accuracy of the model (Figure 7). The intercept, slope, the coefficient of determination (R^2), and both the mean and the standard deviation of the residuals were used for each plot to determine how well the model was able to replicate the stream data based on the selected endmembers. We primarily considered the predictions to be good if the average of the residuals and error was relatively small. The statistics for the fit of the plots can be found on Table 3. The predictions for the Si and K^+ concentrations were less accurate for Woodland and Hailstone relative to Soapstone. Additionally, the model predicted values for $\delta^{18}O$ were underpredicted for Hailstone, the location furthest downstream in the watershed. This is likely due to the limitations of the endmembers selected to describe the chemistry of the full watershed, particularly with the snow endmember. Underpredicted tracers were used as a proxy for inferring the character of unknown endmembers (Foks et al., 2018).

3.4 Comparing mixing calculations using U-space versus tracer space

The maximum difference in fractional contributions for all endmembers calculated in tracer space versus U-space for a three-PC, four-endmember system of equations was between -0.0774 and 0.0978 for Soapstone, -0.0973 and 0.1389 for Woodland, and -0.1229 and 0.1096 for Hailstone (Figure 8, a-c). For the two-PCs, four-endmember case, the maximum differences in fractional contributions between all endmembers was between 0.1181 and 0.2171 for Soapstone,

-0.3187 and 0.3532 for Woodland, and -0.3903 and 0.3831 (Figure 8, d-f). In all locations, the model had more difficulty predicting the carbonate groundwater and soil water contributions for the calculations done in U-space rather than tracer space, primarily during spring runoff.

3.5 Endmember mixing contributions in a nested catchment

Between Soapstone, Woodland, and Hailstone, the endmember contributions vary seasonally and spatially. The groundwater endmembers dominated the water chemistry of each location during winter baseflow (December – February), with quartzite groundwater being the main contributor at Soapstone and carbonate groundwater being the main contributor at Woodland and Hailstone. For Soapstone, Woodland, and Hailstone, the snow endmember increased greatly during spring runoff (April – June), with contributions ranging between 23 - 66%, 21 - 63% and 14 – 60% for each location, respectively (Figure 9 - 11). The average snow input over all the years sampled during spring runoff was 3.9, 5.6, and 7.1 m^3/s for Soapstone, Woodland, and Hailstone, respectively (Figure 12).

3.6 Endmember inputs from upstream to downstream

To quantify the volume of endmember input between locations, the discharge-weighted endmember contributions were subtracted between each location to find the difference in endmember input (Figure 13). Between the Woodland and Hailstone sampling locations, negative volumes were sometimes calculated for the endmembers, with snow most frequently showing negative values. These negative values were interpreted as error in the ability of the endmember to accurately describe the stream data. Also, there were a few cases during summer

where the calculated endmember inputs were negative because discharge was lower at Hailstone due to water diversions between Woodland and Hailstone.

3.7 Estimating error in the endmember datasets

Jackknifing is an important cross-validation technique to use in EMMA to quantify uncertainty caused by the assumption of precisely defined, static endmembers. In the case of Provo River, new datasets of jackknifed endmember averages were calculated for the 9 quartzite groundwater samples, 22 snow samples, 6 soil water samples, and 8 carbonate groundwater samples, which created the same number of averaged groups for each endmember as the number of samples in the respective endmember datasets. Jackknifing the endmember means resulted in 9504 different combinations of the four endmembers, which we used to assess the uncertainty in the fractional endmember contributions of all stream samples (Figure 14).

4. Discussion

4.1 Process for determining conservative tracers

From the bivariate plots (Figure 3), we determined that the conservative tracers for Provo River included $\delta^{18}O$, $\delta^{2}H$, Si, HCO_3^-, Mg^{2+}, K^+, and Ca^{2+}. The choice of which tracers to include in the mixing model is largely subjective, but tracers should only be removed if there is sufficient justification to do so. As a rule of thumb, if the tracer behaves conservatively, then the tracer should be included in the model. The model can only be improved by the inclusion of multiple tracers and helps identify the characteristics of potential missing endmembers (see Section 4.5 - 4.6 below).

4.2 Process for endmember selection using a PCA

EMMA is used to simplify the complex processes of a watershed by using only a few endmembers to model the main inputs. These endmembers are determined using a PCA to visualize the data, where the PCs retained must explain a considerable percentage of variance to accurately determine which endmembers reasonably circumscribe the data. If the mixing is calculated in tracer space, the number of PCs retained dictates the minimum number of endmembers that may be included in the analysis, whereas the maximum number of endmembers is dictated by the number of tracers used in the model to describe the stream data. Performing the mixing calculation in tracer space allows for the inclusion of more endmembers than would be allowed in U-space, allowing the user to make their model potentially more complex.

The minimum number of endmembers that can be used in EMMA is the number of PCs used to explain the stream data plus one, as this is the number of points required to define a convex hull. Using the minimum number of endmembers can be used to describe the basic processes occurring in the watershed and is the more common approach to apply EMMA. The model could be made more complex by including additional endmembers, and these endmembers may also be screened using a PCA. However, it may be necessary to observe how well the endmembers circumscribe the data in U-space with additional PCs to ensure that the endmembers are distinct from each other. In the case of Provo River, the potential endmembers were projected into U-space and the snow, quartzite groundwater, and carbonate groundwater endmembers sufficiently circumscribed the stream data in 2D space. However, previous studies of the Provo River watershed showed that soil water as an important contributor (Checketts et al., 2020; Hale et al., 2022). In U-space, the soil water endmember plotted between the snow and carbonate groundwater endmembers, seeming to indicate it could be treated as a simple mixture

of the two endmembers. To confirm whether soil water had distinct behavior from the other endmembers, the stream data and potential endmembers were projected into 3D space (Figure 5). Viewing the spread of data in 3D made it clear that soil water would be an important endmember to include to describe the stream data, which was not apparent in the previous 2D model. This was then confirmed with the raw tracer data, where soil water was uniquely enriched in Si and K in comparison to the other endmembers.

There is also a limit in EMMA to the maximum number of endmembers that may be included. The maximum number of endmembers that may be included is equal to the number of tracers being used in the analysis to avoid creating an underdetermined system of equations. Using an equal number of endmembers to tracers would result in a critically determined system of equations, producing a unique solution. Including more endmembers than tracers in the model would result in an underdetermined system of equations, which typically results in an infinite number of solutions, but may be solvable depending on the shape of the function and if proper constraints are put on the solution (Butt, 2011). It is likely that there is no unique solution in an overdetermined system, but a least-squares, best-fit solution can typically be found which has the advantage over an underdetermined system by being constrained by more variables (Gentle, 1998).

In terms of calculating the mixing in U-space, the maximum and minimum number of endmembers that may be included are directly restricted to the number of PCs retained. Since the mixing is calculated using the PC scores, the maximum number of endmembers that may be included is the number of PCs retained plus one, as including more endmembers would result in an underdetermined system. In this approach, many studies usually perform the calculation in U-space using the minimum number of endmembers, creating a critically determined system of

equations (Chisola et al., 2022; Montagud et al., 2021; Wilson et al., 2016). Performing this calculation using the PC scores is solvable, but considerable error could be introduced into the results as the PC scores contain only a fraction of the original information (this will be explained in the next section).

4.3 Improved mixing calculations using tracer space instead of U-space

After determining the tracers and endmembers to use in the analysis, the fractional contributions may be calculated. Calculating the mixing in tracer space rather than in U-space allows for the inclusion of more information and thus more accurate results. The main problems involved with performing the mixing in U-space are that the optimization is constrained using less information, and that the number of endmembers that may be selected is more limited. Calculating the mixing in U-space without using all of the PC scores will result in the calculation being done with only a fraction of the information, which could cause the fractional contributions to be less accurate. Fractional contributions calculated in U-space may be comparable to those calculated in tracer space, but the accuracy of the U-space calculation is heavily dependent on how much information is retained by the principal components and how well the endmembers circumscribe the data. This makes the use of a PCA an important and effective tool for screening potential endmembers, but not as accurate for calculating the fractional contributions themselves. We can then assume a priori that calculating inside of tracer space is more reliable than calculating in U-space because the optimization is constrained using more information.

In the case of Provo River, the fractional contributions were calculated in three different cases: a two PC and four endmember model, a three PC and four endmember model, and a seven

tracer and four endmember model. In the two PC and four endmember model, the accuracy in the predictions deviate significantly from the results calculated in tracer space using four endmembers. Since the system of equations was underdetermined, the fractional contributions, particularly for carbonate groundwater and soil water, were not predicted well by the model (Figure 7, a-c). In the three PC and four endmember model, the estimated fractional contributions became far more accurately represented by the model compared to the previous case, but there are still deviations between the values calculated in tracer space rather than in 3D U-space (Figure 7, d-f). We can assume that deviations in the calculation occur from the calculations done in U-space because the optimization would be constrained on a fewer number of variables than in tracer space. This makes calculating the mixing in tracer space the best approach to retaining the maximum amount of information for both simple and complex models.

4.4 Using jackknifing to calculate error in the EMMA model

The results from jackknifing the mean endmember compositions suggest that there is little error caused by the distribution of the data in the endmember samples themselves and that the removal of an individual sample in the group did not strongly control the results of the mixing model. The greatest amount of error observed in Soapstone was with the carbonate groundwater endmember, likely because of the difficulty that the model might have had constraining the differences between soil water and carbonate groundwater for the enrichment in the higher part of the watershed. With Woodland and Hailstone, the largest errors were calculated for the snow endmember because differences between the snow and quartzite groundwater endmembers were largely due to the isotopic ratios, and there may have been more isotopically enriched snow input further downstream that were not sampled.

4.5 Application of EMMA to a nested catchment

Standard error calculation, such as the jackknifing method, only addresses error within the endmember samples themselves. However, they cannot address the more fundamental problems such as the fact that simplifying the water input to a complex watershed to only a few endmembers will unavoidably introduce error. Because the application of EMMA is necessarily a simplification, calculating plausible results does not necessarily equate with correct results. In fact, it is always incorrect to some degree because any real system is more complicated than the EMMA model. However, performing EMMA in a nested catchment can make it easier to infer the nature of possible sources of error by identifying which location in the catchment is best described by the selected endmembers, and in turn identify those areas where additional endmembers are required. EMMA can additionally produce results that help to understand the relative inputs of endmembers between locations throughout a watershed. These errors can be assessed by identifying underpredicted or overpredicted model values, and the relative endmember inputs between locations.

4.5.1 EMMA produced plausible results for the Provo River watershed

The fractional contributions of the endmembers at the three locations in Provo River were quite plausible when viewed individually. Between the three sampling locations, strong seasonal variability was observed in the fractional contributions of quartzite groundwater, snow, soil water, and carbonate groundwater. Baseflow was dominated by the groundwater components most associated with the geology upstream from the sampling sites, i.e., quartzite groundwater dominated at Soapstone and carbonate groundwater dominated at Woodland and Hailstone. The

increase in the snow fraction for all locations correlated with peak runoff, but the total volume of snow input into the stream each year was difficult to quantify. The 2017 water year had relatively high snowpack, which was reflected in increased calculated fractional contributions of snow, but similar trends were seen in 2020, which was a below-average snowpack year. Thus, snowpack volumes do not necessarily indicate a year of high runoff or snow input because antecedent soil moisture and air temperature also control how much snowmelt makes it directly into the stream without significant soil interaction (Brooks et al., 2021). Additionally, the increased calculated input of soil water and quartzite groundwater at Woodland is likely due to the input from the North Fork of the Provo River, a major tributary to the upper Provo located between Soapstone and Woodland (Figure 1). Likewise, the increased input of soil water and quartzite groundwater to Hailstone is likely due to inputs from the Weber-Provo Diversion Canal.

4.5.2 Identifying limitations in the nested catchment approach by observing the accuracy of model predicted values and endmember inputs between locations

To determine whether the selected endmembers can describe the chemistry at several points of interest along a watershed, the predicted model concentrations can be assessed for missing endmembers. A limitation in the nested catchment approach is that only a few endmembers can be selected to explain the stream data at all locations of the watershed. To apply the model to the whole watershed, the endmembers that are observed at the bottom of the watershed must also be observed at the top of the watershed. In the case of the Provo River watershed, most of the endmembers were identified from the geology in the area, except for the groundwater that had interacted with volcanic bedrock in the lower part of the watershed.

Previous studies of Provo River found little evidence of pronounced solute loading from groundwater interactions with volcanic rock (Carling et al., 2015; Checketts et al., 2020), so this potential endmember was ignored. Using a volcanic groundwater endmember would have excluded Soapstone from the model because there is no volcanic rock above this site. After running EMMA on the dataset, Soapstone was well predicted for all tracers by the selected endmembers. However, the accuracy of the predicted concentrations of Si and K^+, and to a lesser extent Mg^{2+}, became increasingly poor between Woodland and Hailstone. This suggests the necessity for an additional endmember, perhaps a volcanic groundwater endmember, to explain the chemistry at Woodland and especially Hailstone. This approach can be used as a preliminary assessment to determine whether there are any missing endmembers at multiple points along the watershed.

One way to assess the accuracy of the calculated fractional contributions is to calculate the net increase in endmember contributions between successive sampling locations downstream in the catchment. The endmember inputs between locations were calculated by subtracting the discharge-weighted contributions between locations to determine what the inputs were. For Provo River, the fractional contributions alone for each location gave realistic and interpretable results. However, viewing the data in terms of the endmember inputs into successive locations downstream produced some negative values, indicating error within the analysis since it is impossible that a single endmember source would be lost in the stream between sampling points. The endmember that appeared most frequently as a negative input was snow, particularly between Woodland and Hailstone. This could be a result of increasing complexity in the watershed from upstream to downstream with a greater likelihood that additional water sources

would affect downstream locations and confound mixing calculations based on a now insufficient set of endmembers.

The difficulty in accurately quantifying snow input to the downstream locations could be caused by two different factors. First, isotopically enriched snow sources lower in the watershed could confound the mixing calculations with respect to snow and quartzite groundwater. The snow and quartzite groundwater endmembers are primarily distinguishable by their isotopic composition, with snow being more depleted in the heavy $\delta^{18}O$ and $\delta^{2}H$ isotopes. Therefore, an influx of isotopically enriched snowmelt would be interpreted by the mixing model as having a larger fraction of quartzite groundwater, and a smaller fraction of snow, than is actually the case. This would manifest as a negative contribution for the snow endmember between locations in Figure 12. This interpretation is supported by the fact that our snow endmember samples were only collected in one of the highest parts of the watershed. The snow input estimates are the poorest between Woodland and Hailstone, and it should be noted that the Weber Diversion provides some input of water there. Although that watershed is geologically similar to the Provo River watershed, it may be that the snow there is isotopically distinct, on average. Second, mixing with other, previously undetected endmembers might produce a similar effect. Our proposed volcanic groundwater endmember is a likely contributor.

Considering the endmembers selected to represent the whole watershed, there is much room for improvement. Generally, the calculation overall could be improved by including more representative endmember samples. For Provo River, it appears that EMMA may be best suited for Soapstone, the upstream site with the simplest watershed characteristics. An advantage of the nested catchment analysis in Provo River is that the model produced plausible results, and using this approach, we can identify how useful the interpretations are based on the assumptions made.

A nested catchment analysis can help with identifying error present in EMMA throughout the watershed than would have been noticed in measuring the mixing at only one location.

4.6 Quantifying differences in predicted solute concentrations to identify missing endmembers

Fractional contributions from the mixing calculations can be used to calculate predicted values for other tracers not included in the analysis to identify missing endmembers. The values for several of the commonly conservative elements that were not included in our mixing model, specifically Na^+ and Cl^-, were used to predict concentrations. For the Provo River, both of these tracers were significantly underpredicted for Woodland and Hailstone but not for Soapstone, suggesting a missing endmember such as road salt in the model. Because the roads are regularly maintained in the lower parts of the watershed, we would expect a larger input of road salt further downstream in the watershed. The industry standard for road salt is ~50 kg of salt per km per lane. Based on the total amounts of salt used to maintain the roads in Kamas and the lengths of road maintained, there can be anywhere between 6 – 12 metric tons of salt placed on a single lane of road 1 km long over an entire winter season. These rough estimates suggest that the underpredicted values of Na^+ and Cl^- for the lower parts of the watershed are due to the addition of road salt, making salt a missing endmember for Woodland and Hailstone. Salt maintenance and total salt usage from 2015 – 2023 was obtained from the Utah Department of Transportation (personal communication).

4.7 Suggested workflow for applying EMMA models

Considering the multitude of approaches in the literature for building an EMMA model for a watershed, we suggest a streamlined workflow that minimizes error and identifies missing endmembers, as follows:

1. Collect stream and endmember samples for the area of interest. To better understand the error associated within the EMMA calculation, the stream should be sampled in multiple locations along the watershed to compare the spatial changes in stream chemistry over time. However, if limitations do not allow multiple sampling locations, EMMA may still be performed on stream samples collected in a single location.
2. Determine which elements included in the dataset behave conservatively. One should be aware of the fundamentally different processes affecting isotopes and solutes and make general assumptions about the behavior of the isotopes to determine if they should be included in the analysis.
3. Standardize (z-score) the stream data and perform a PCA. Determine the number of PCs to include by observing eigenvalues (see "rule of one"), structure in residual values for each tracer, and the percent variance explained by each PC. The selection of PCs is a largely subjective choice, but one should provide justification for the number of PCs selected and ensure that they explain a reasonable amount of variation in the dataset.
4. Project potential endmembers into the stream data-defined U-space. Endmembers should be z-scored using the mean and standard deviation of the tracers in the stream data and PC scores calculated using the coefficient matrix of the stream data. Select endmembers to use in the mixing analysis based on how well the endmembers circumscribe the stream data in U-space.

5. Perform the mixing calculation by using a non-negative least-squares optimization using z-scored tracer values for both the stream and endmember data. Ideally, the system of equations should be either critically determined or overdetermined.

5. Conclusion

An endmember mixing analysis is a useful tool for understanding how the main water sources for a stream change over time. However, it is important to highlight that EMMA is inherently an oversimplification of real processes occurring within a watershed. Many assumptions must be included for the analysis to be possible, including that the mixture is composed of a small number of endmembers, and that these endmembers have fixed concentrations over time. In reality, natural systems are often far more complex, but the use of EMMA can still be useful depending on the intention of the user. Applying EMMA to a nested catchment allows for further assessment of the error present in the analysis. The application of EMMA to the Provo River shows that the lowest part of the watershed, Hailstone, is the most poorly represented by the model because the watershed becomes increasingly complex further downstream. This approach validates the application of these endmembers to the highest sampling location, Soapstone, and suggests additional endmembers that may be required to accurately describe the chemistry of Woodland and Hailstone. By calculating the mixing in tracer space and testing the selected endmembers at multiple locations in the watershed, the error in the already simplified EMMA may be minimized and yield more reliable and interpretable results.

6. Tables

Table 1. Table of river samples collected over the five-year study. All samples from each location (Soapstone, Woodland, and Hailstone), so the samples shown in the table represent the samples collected for one site. Between all locations, 318 samples were collected.

	Number of Samples Collected (per location)					
	2016	**2017**	**2018**	**2021**	**2022**	**Total**
Spring Runoff (April – June)	11	11	12	12	14	60
Other	9	7	8	10	12	46
Total:	20	18	20	22	26	106

Table 2. Values from the coefficient matrix for the river data. Three PCs were used to observe the river data and select endmembers, with particular weight being on the solutes for PC1, the isotopes for PC2, and Si for PC3.

	PC1	**PC2**	**PC3**	**PC4**	**PC5**	**PC6**	**PC7**
$\delta^{18}O$	-0.09	**0.71**	0.31	-0.59	-0.21	-0.01	0.08
$\delta^{2}H$	-0.12	**0.69**	-0.31	0.60	0.23	0.01	-0.04
HCO_3^-	**0.45**	0.08	-0.31	-0.13	-0.19	0.73	-0.32
Si	**0.42**	0.06	**0.70**	0.49	-0.30	0.04	-0.01
Mg^{2+}	**0.45**	0.08	-0.27	-0.09	-0.20	-0.67	-0.47
K^+	**0.44**	0.06	0.23	-0.19	0.85	0.00	-0.03
Ca^{2+}	**0.45**	0.05	-0.31	-0.02	-0.13	-0.09	0.82

Table 3. Statistics associated with the fit between the model predicted concentrations and observed concentrations.

	R^2	**Slope-1**	**Intercept**	**Residual Average**	**Standard Deviation Average**
$\delta^{18}O$	0.78	-0.32	-5.50	0.23	0.35
$\delta^{2}H$	0.90	0.03	4.00	0.02	1.28
HCO_3^-	0.98	-0.13	3.50	4.11	7.49
Si	0.75	-0.54	1.40	0.15	0.82
Mg^{2+}	0.98	-0.22	0.26	0.52	0.61
K^+	0.71	-0.49	0.20	0.10	0.14
Ca^{2+}	0.99	0.06	-0.03	-0.82	1.26

Table 4. Location in UTM coordinates and dates for each endmember sample collected. All soil water and carbonate groundwater samples were collected in 2022.

Sample Name	**Date Collected**	**UTM Zone**	**Easting**	**Northing**
Quartzite Groundwater				
UP-Spring 1	10/31/12	12T	507249	4504617
UP-Spring 1	10/18/13	12T	507012	4504770
UP-Spring 1	10/31/14	12T	507249	4504617
UP-Spring 2	10/31/12	12T	506890	4504998
UP-Spring 2	10/18/13	12T	506890	4504998
UP-Spring 2	10/31/14	12T	506890	4504998
POF 8	5/26/16	12T		
UP-Spring 1	10/14/22	12T	507249	4504617
UP-Spring 2	10/14/22	12T	506890	4504998
Carbonate Groundwater				
Carbonate Spring 1	8/5/22	12T	496962	4482869
Carbonate Spring 2	8/5/22	12T	492228	4488303
Carbonate Spring 1	9/23/22	12T	496962	4482869
Carbonate Spring 2	9/23/22	12T	492228	4488303
Carbonate Spring 1	10/19/22	12T	496962	4482869
Carbonate Spring 2	10/19/22	12T	492228	4488303
Wolf Creek Spring	10/19/22	12T	499446	4481797
Carbonate Spring 2	11/18/22	12T	492228	4488303
Soil Water				
2022 Soil 1	5/24/22	12T	504211	4498719
2022 Soil 2	6/2/22	12T	508406	4503991
2022 Soil 3	6/2/22	12T	507099	4503477
2022 Soil 4	6/2/22	12T	507153	4503482
2022 Soil 5	6/2/22	12T	507194	4503488
2022 Soil 6	6/2/22	12T	506061	4503637
2022 Soil 7	6/2/22	12T	506040	4503623
2022 Soil 8	6/2/22	12T	503897	4502921
2022 Soil 9	6/2/22	12T	503909	4502934

Snow				
Snow 1-A	4/19/21	12T		
Snow 1-B	4/19/21	12T		
Snow 1-C	4/19/21	12T		
Snow 2-A	4/19/21	12T		
Snow 2-B	4/19/21	12T		
Snow 2-C	4/19/21	12T		
Trial Lake-2B	4/29/16	12T	507333	4503767
Trial Lake-2C	4/29/16	12T	507333	4503767
Trial Lake 3	4/21/17	12T	507202	4503903
Trial Lake 6	4/21/17	12T	502897	4503584
Uinta Snow 1A	4/24/18	12T	507287	4503790
Uinta Snow 1B	4/24/18	12T	507287	4503790
Uinta Snow 1C	4/24/18	12T	507287	4503790
Uinta Snow 2A	4/24/18	12T	503265	4502665
Uinta Snow 2B	4/24/18	12T	503265	4502665
Uinta Snow 2C	4/24/18	12T	503265	4502665
Trial Lake 2	3/25/14	12T	504379	4503049
Trial Lake 3	3/25/14	12T	504379	4503049
Beaver Divide 1	3/25/14	12T	491727	4495728
Soapstone 3	3/25/14	12T	496313	4491481
Trial Lake 4	4/24/14	12T	507089	4504010
Trial Lake 7	4/24/14	12T	502643	4503861

7. Figures

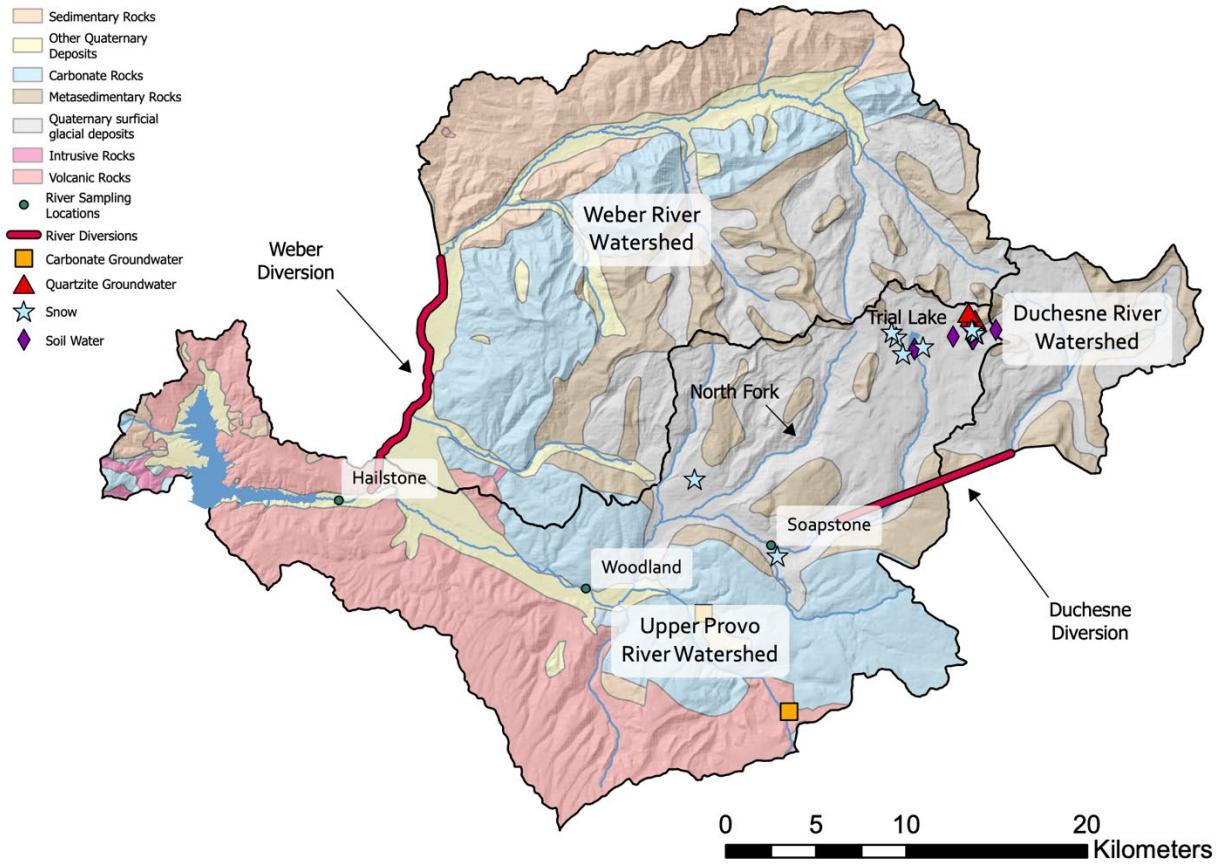

Figure 1. Delineated watershed boundaries for Weber, Duchesne and upper Provo rivers, showing river sampling sites and endmember sampling sites. Geologic map modified after http://geology.utah.gov/map-pub/maps/gis/, obtained 26 April 2023.

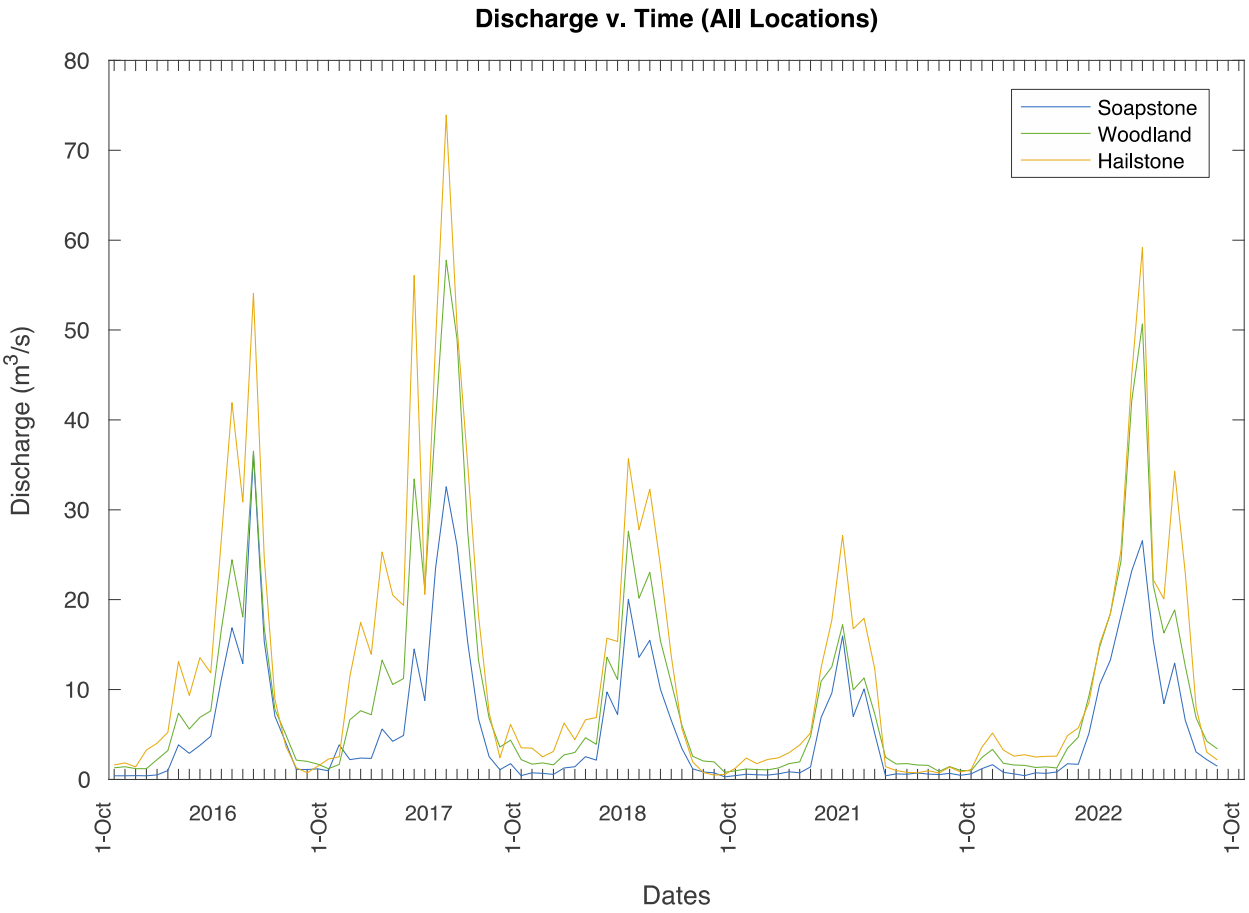

Figure 2. Plot of discharge rates in m^3/s for Provo River at the three separate sampling locations.

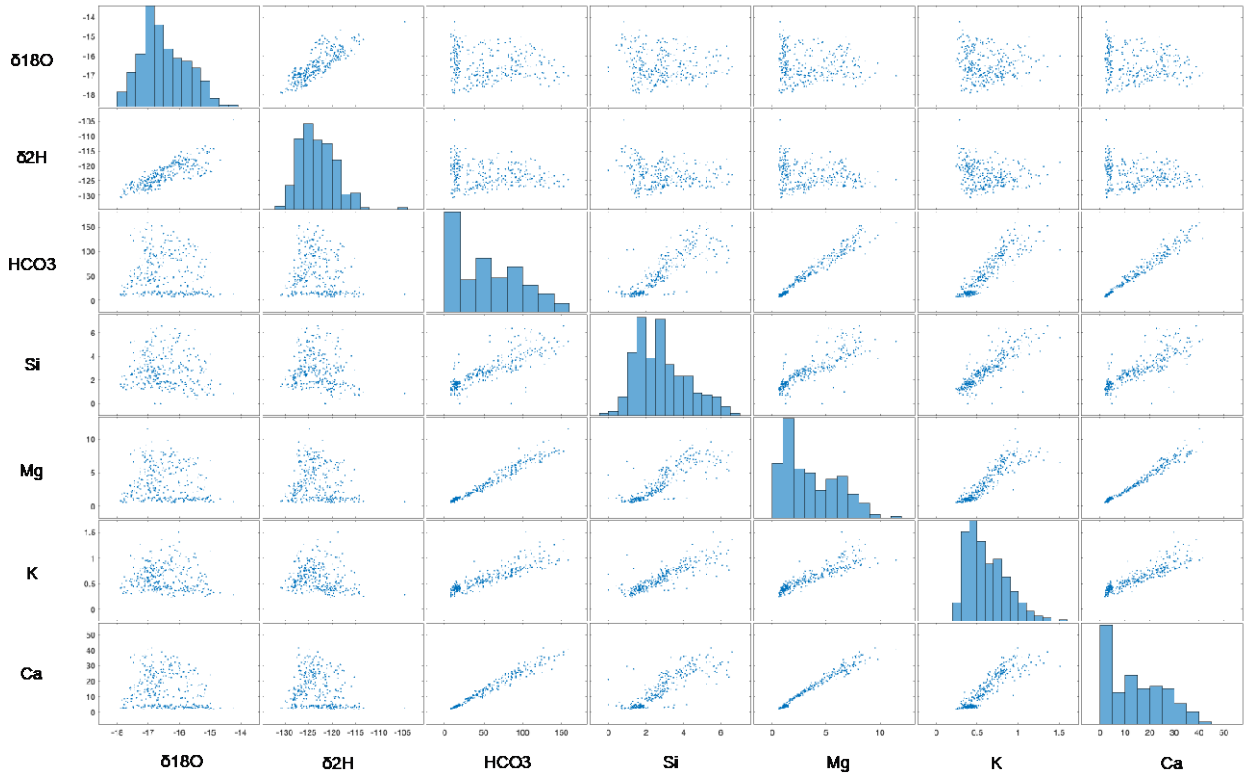

Figure 3. Bivariate plots of the tracers used in EMMA for Provo River. Each solute was strongly correlated with each other ($R > 0.80$).

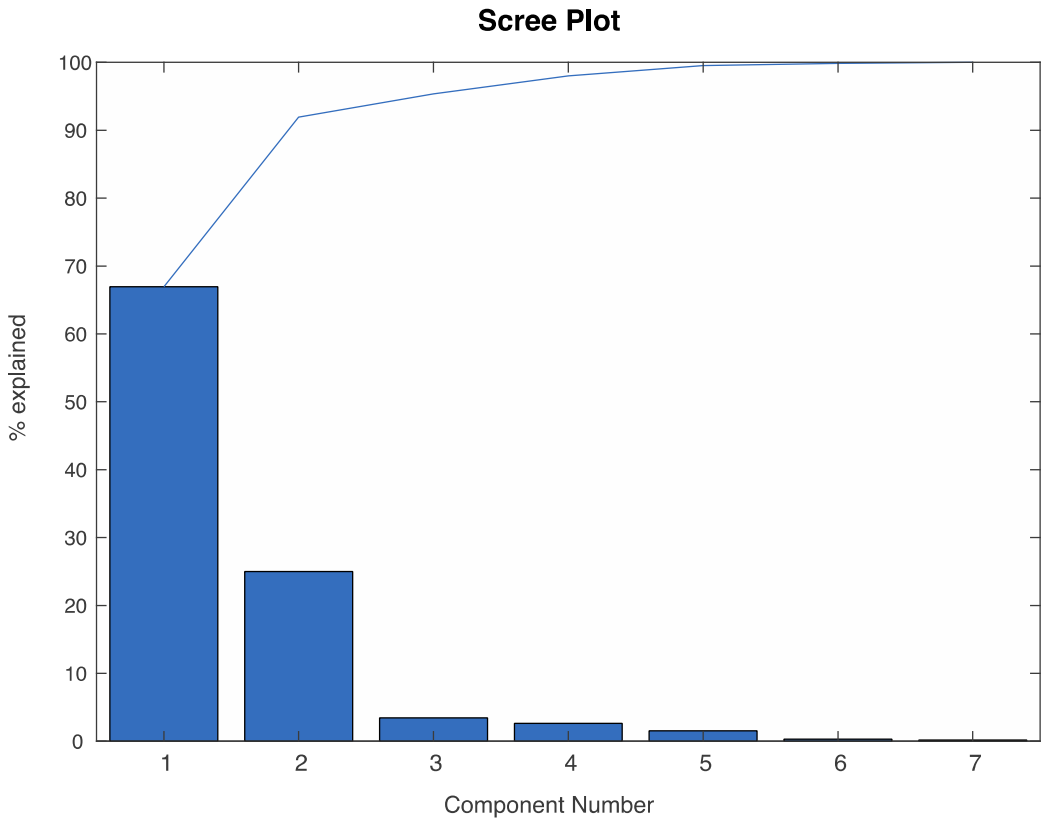

Figure 4. Scree plot from Provo River PCA, indicating a two PC model to sufficiently describe the variance in the dataset.

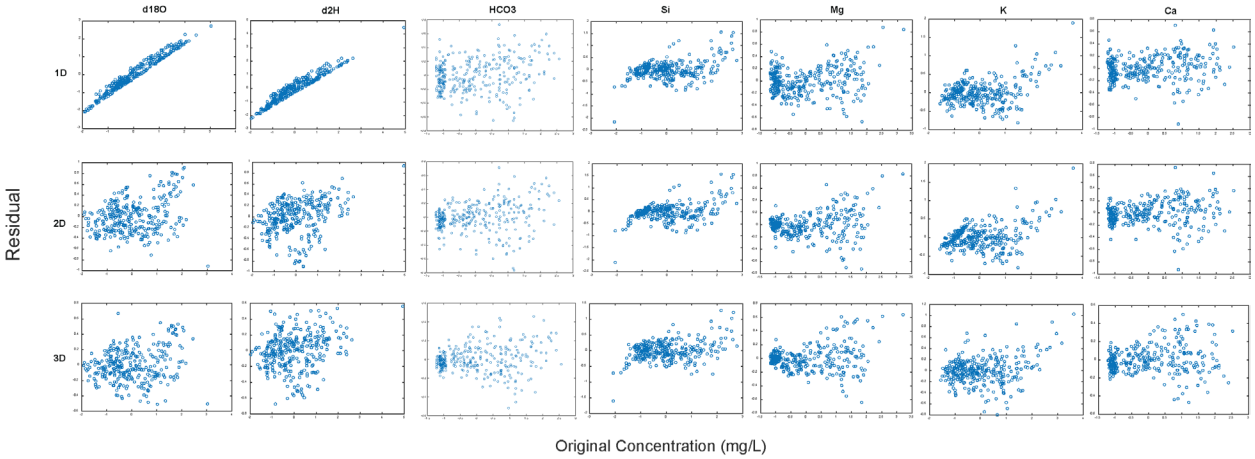

Figure 5. Residual plots for each tracer in 1D, 2D and 3D U-space. Structure in the residuals, particularly for the isotopes $\delta^{18}O$ and $\delta^{2}H$, improve significantly between a one PC and a two PC model, with little change in the structure for all tracers between a two PC and a three PC model.

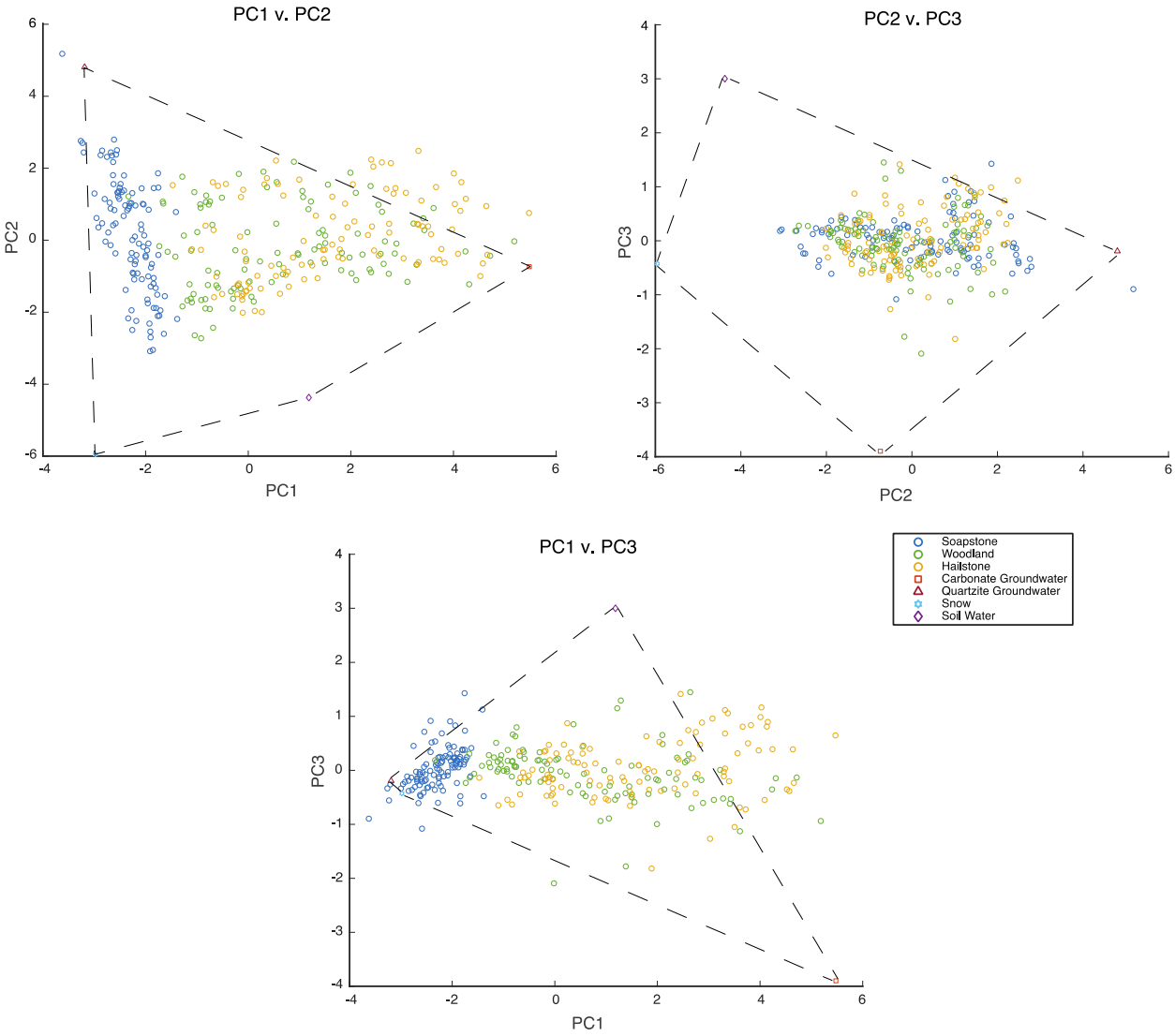

Figure 6. Provo River data plotted in terms of the first, second, and third principal components, with PC1, PC2, and PC3 explaining 66.9%, 25.0%, and 3.4% of the total variance. The endmembers which adequately circumscribe the data are quartzite groundwater, snow, soil water, and carbonate groundwater.

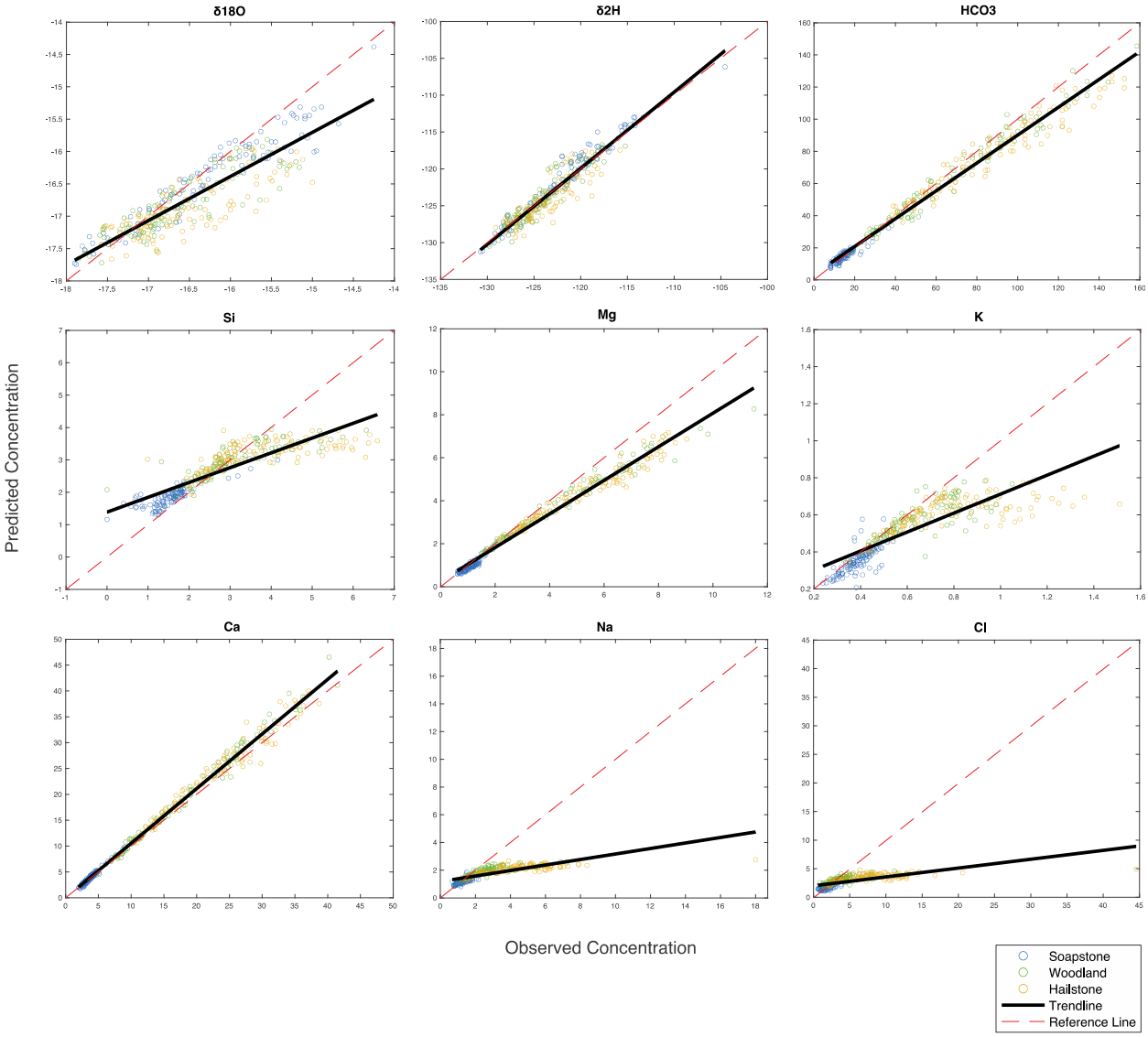

Figure 7. Model predicted concentrations versus observed concentrations for the Provo River data. Na^+ and Cl^- model predictions were used to observe how well the selected endmembers could explain these solutes to determine a missing endmember.

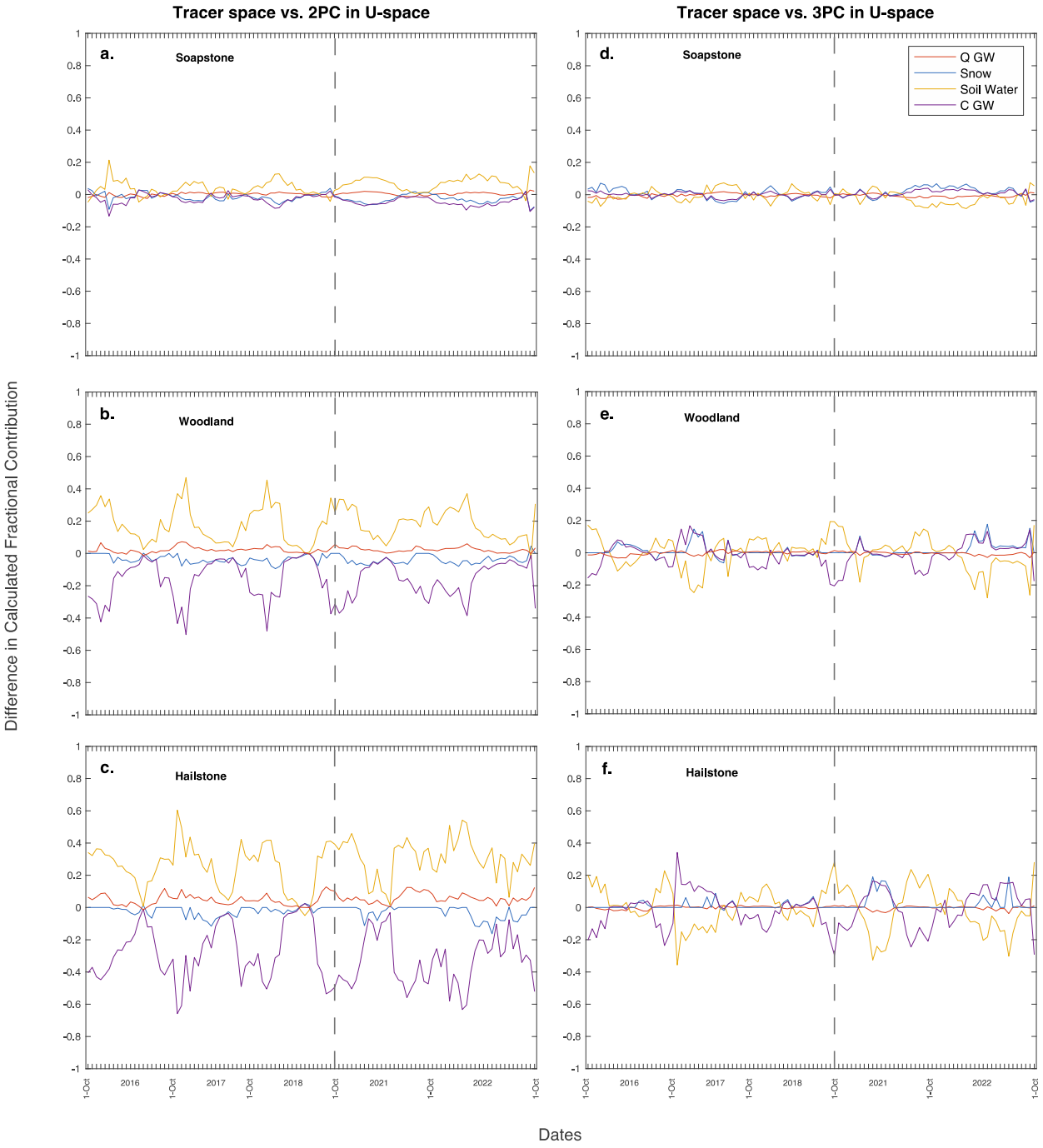

Figure 8. (a – c) Plots of the fractional contributions calculated in tracer space subtracted by the contributions calculated in U-space using two PCs and four endmembers. (d – f) Plots of the fractional contributions calculated in tracer space subtracted by the contributions calculated in U-space using three PCs and four endmembers. Dashed line indicates two-year break in sampling collection.

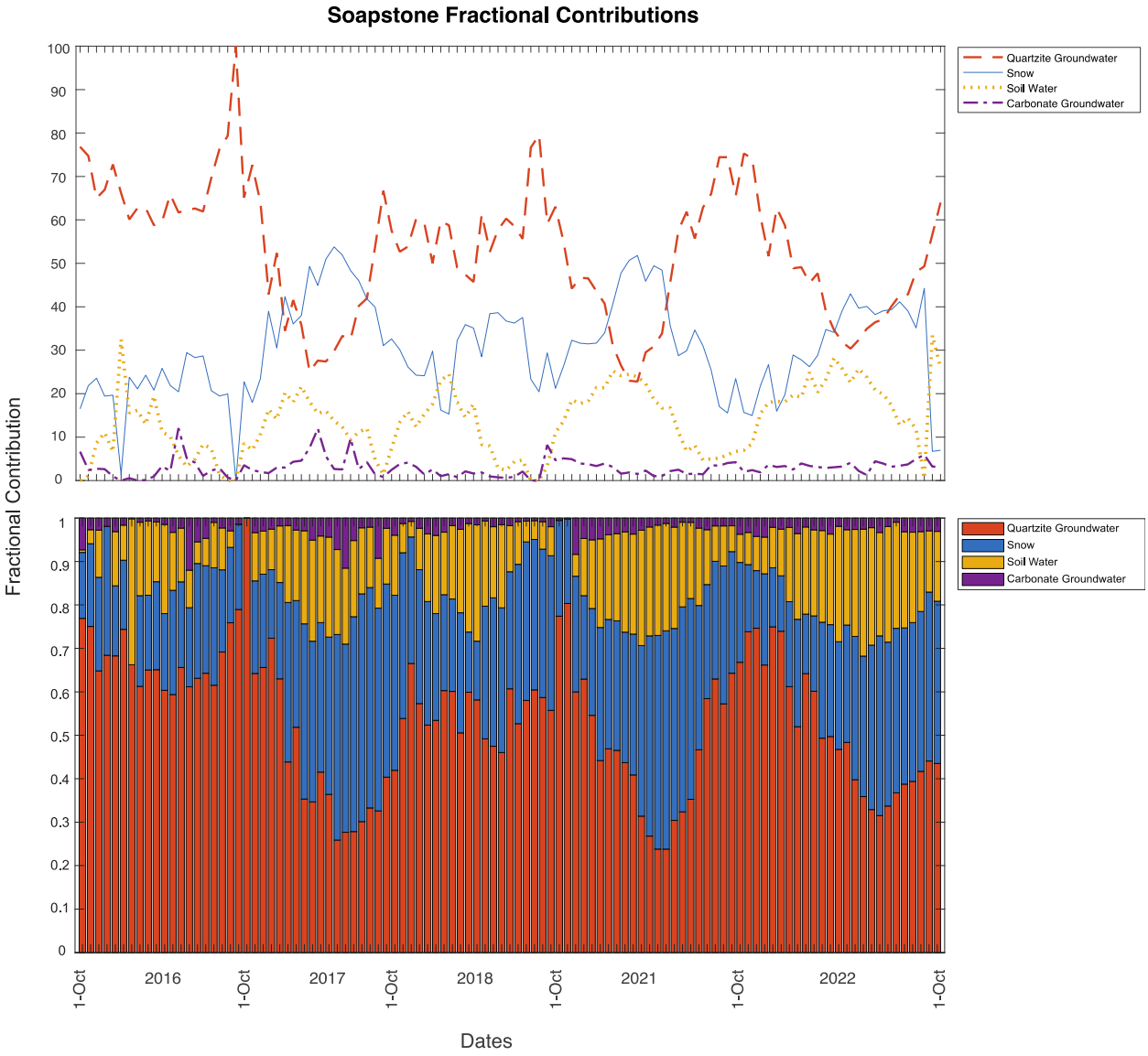

Figure 9. Fractional contributions from each endmember for Soapstone for the time period 2016 – 2018 and 2021 – 2022.

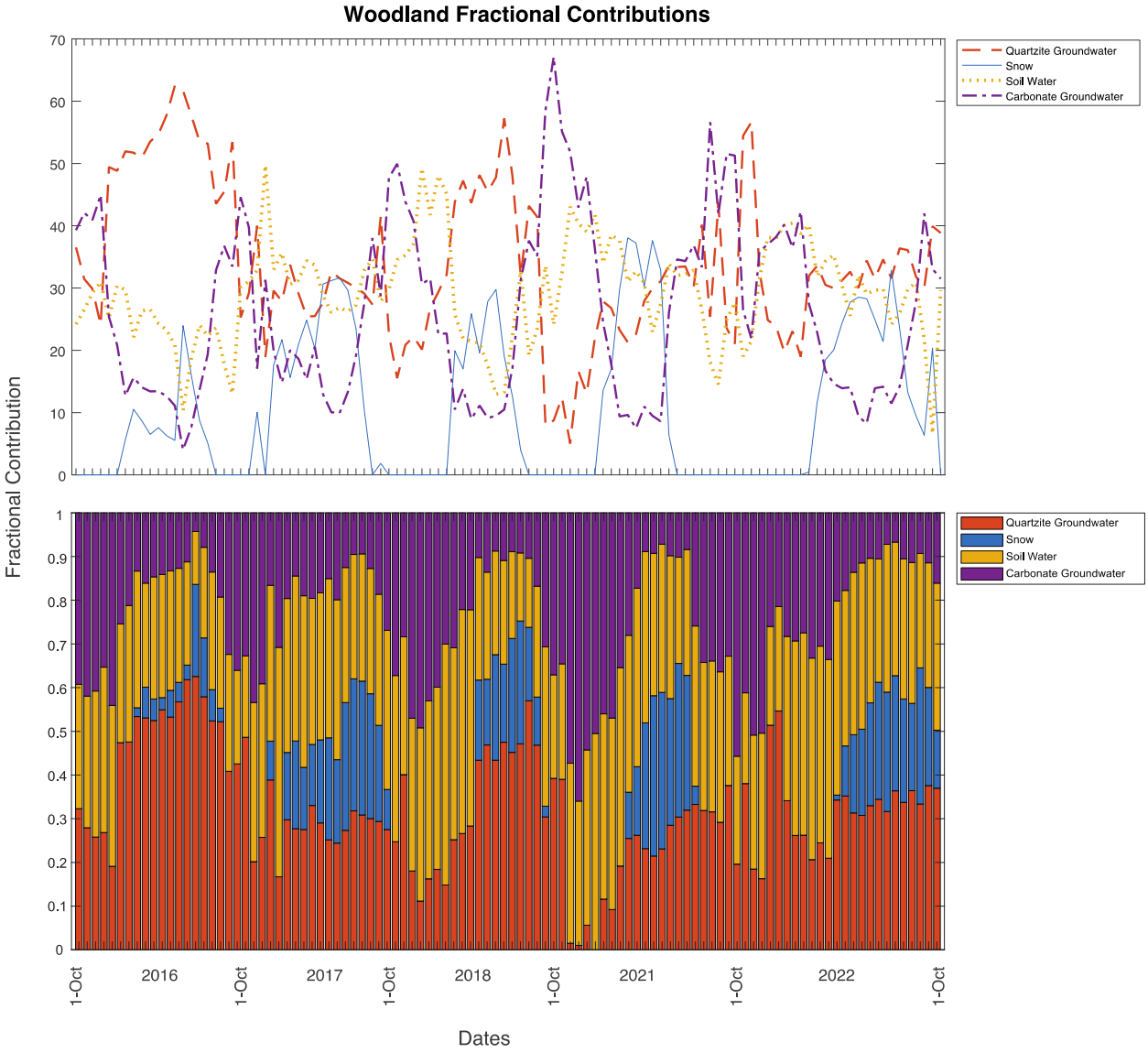

Figure 10. Fractional contributions from each endmember for Woodland for the time period 2016 – 2018 and 2021 – 2022.

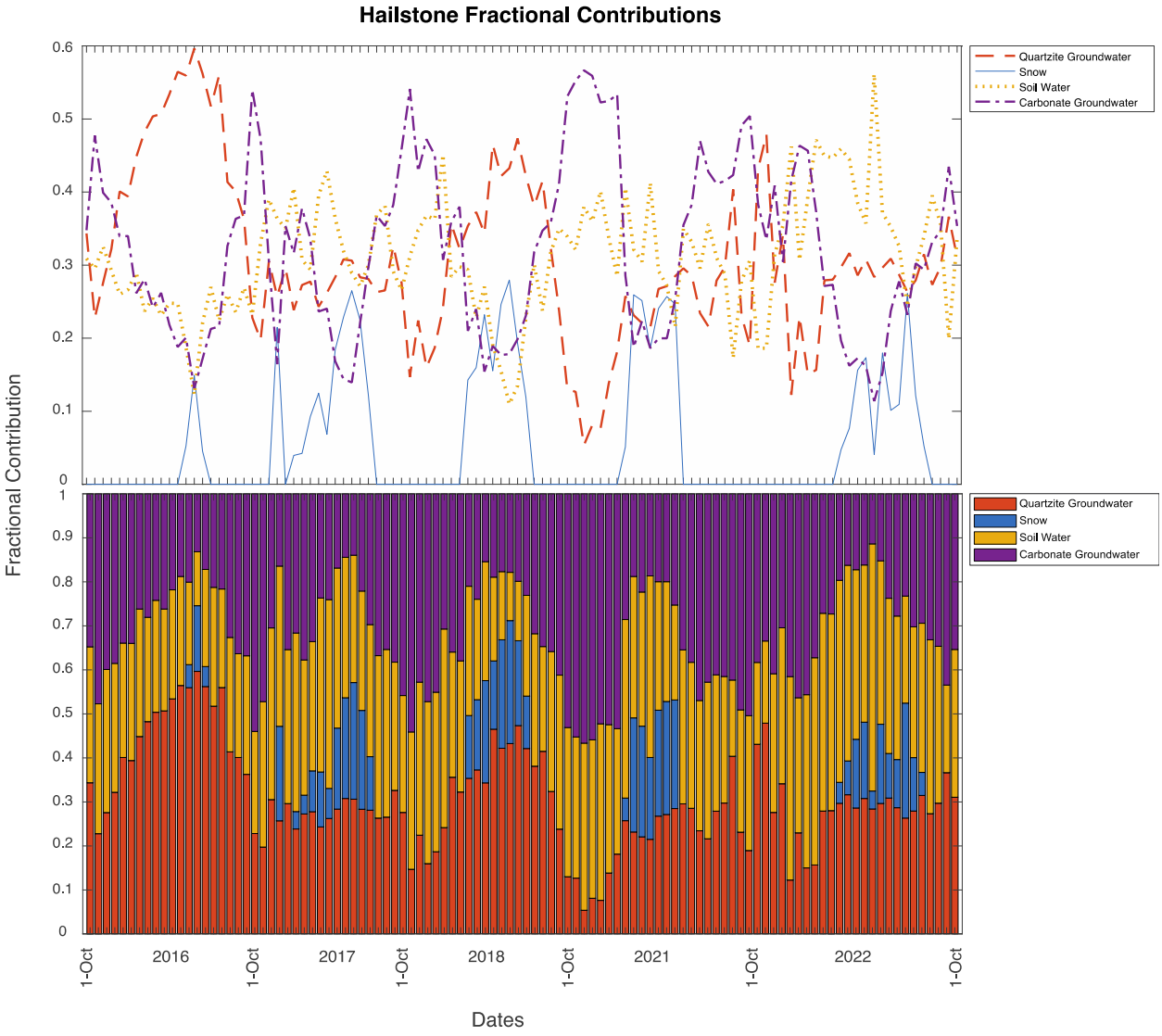

Figure 11. Fractional contributions from each endmember for Hailstone for the time period 2016 – 2018 and 2021 – 2022.

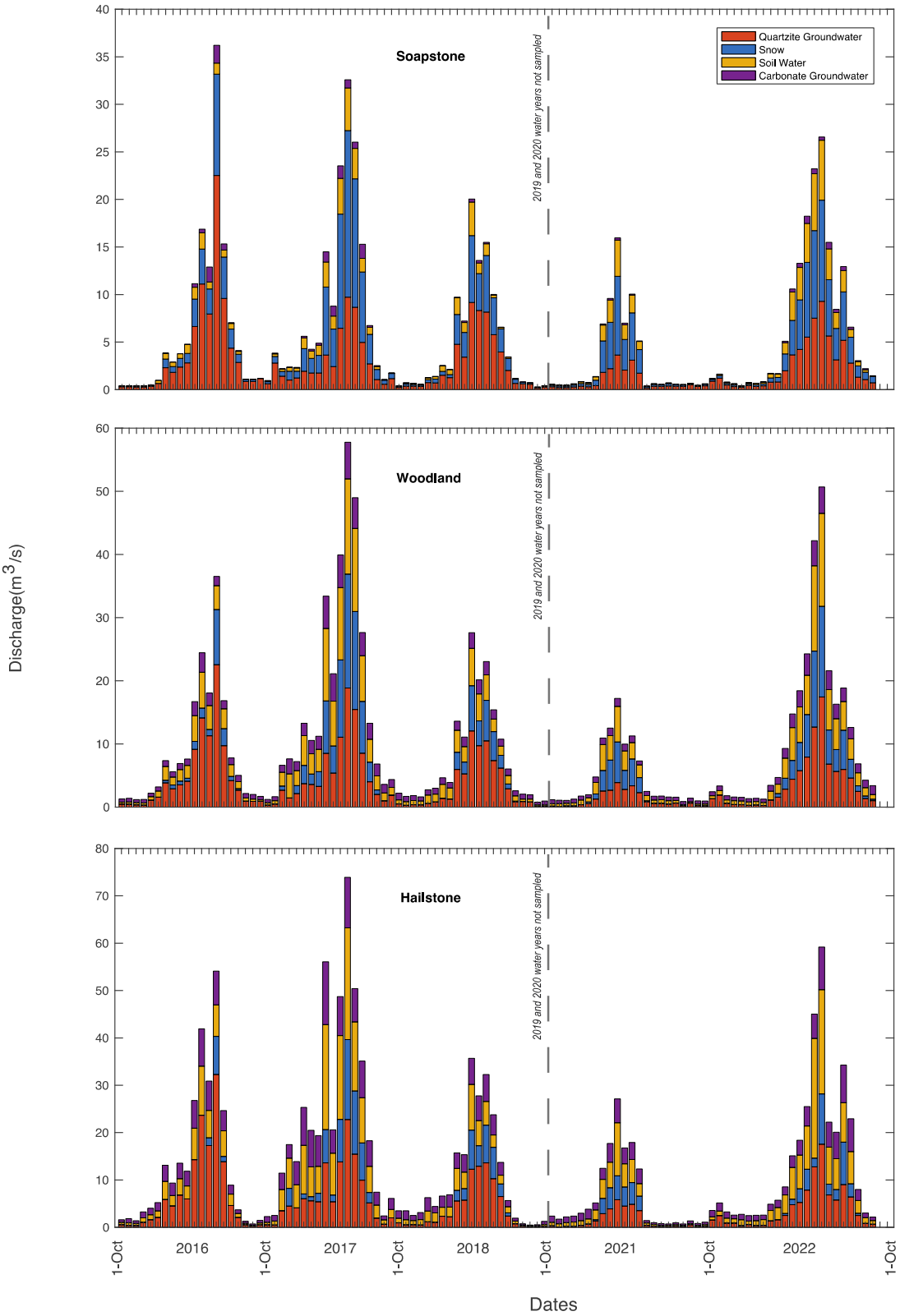

Figure 12. Discharge weighted fractional contributions in m^3/sec for Soapstone, Woodland, and Hailstone, respectively.

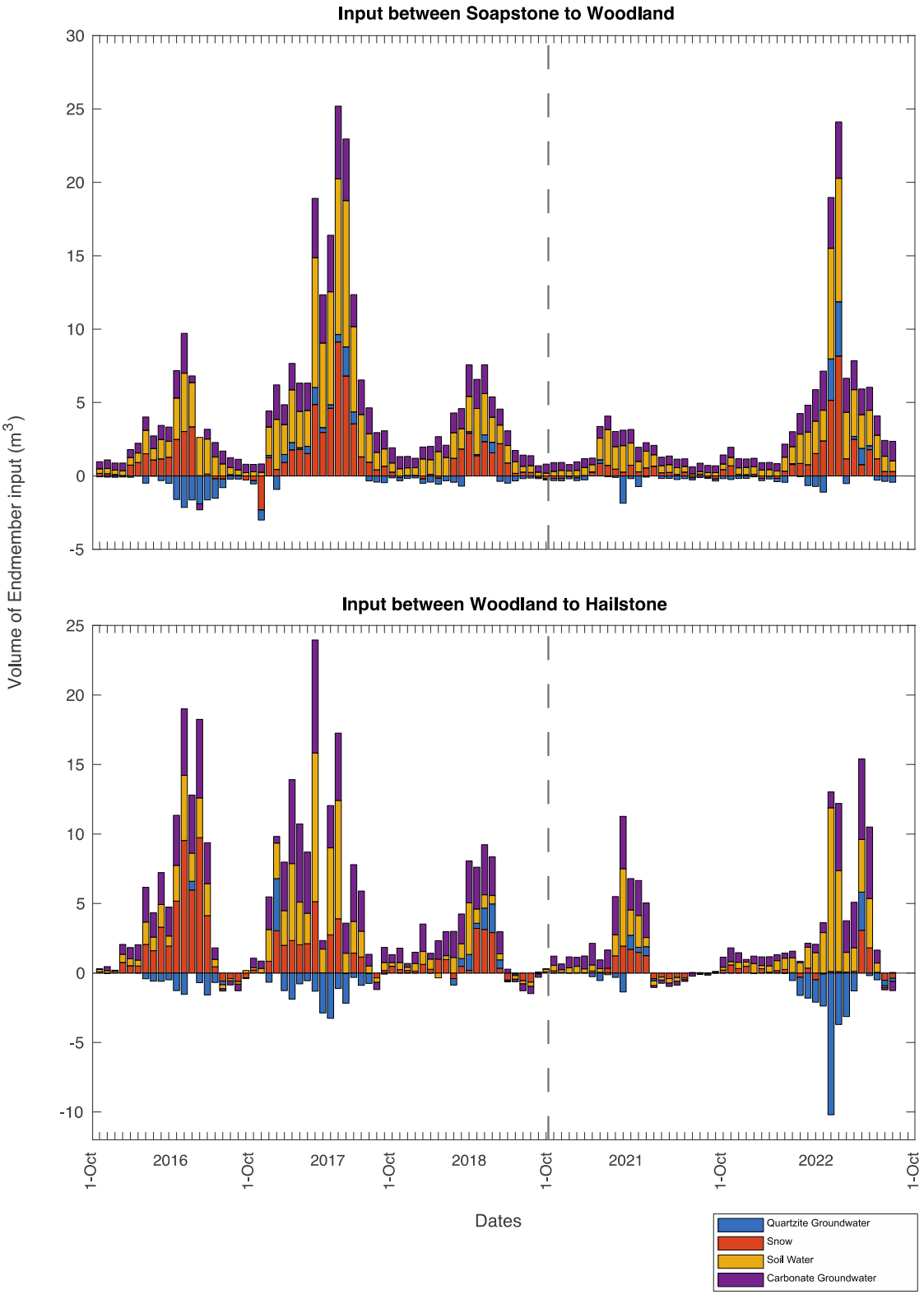

Figure 13. Endmember inputs between locations in the Provo River watershed.

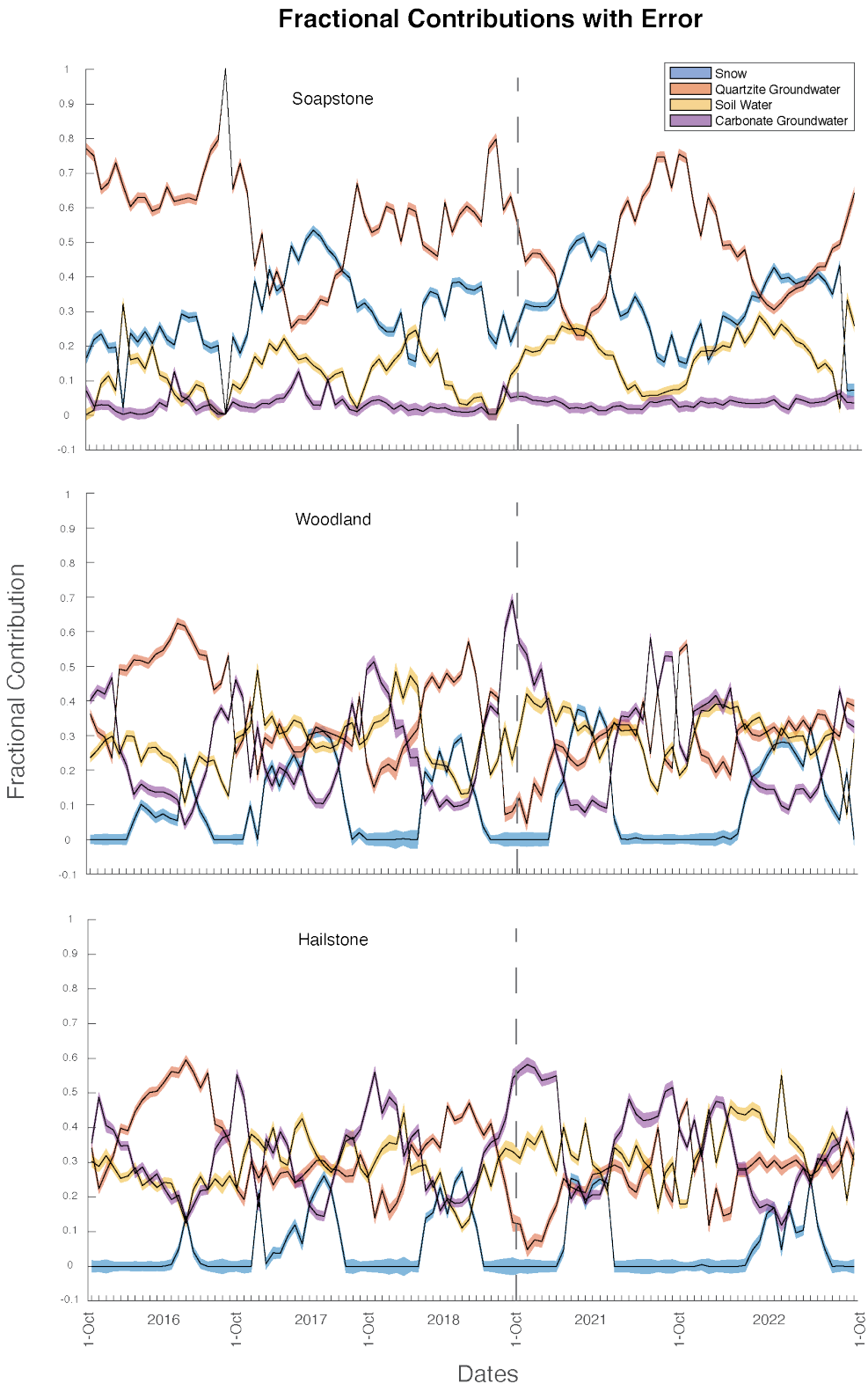

Figure 14. Error within endmember sampling groups for each sampling day between all sampling locations.

8. References

Albarède, F. (2009). *Geochemistry: An Introduction* (2nd ed.). Cambridge University Press. https://doi.org/10.1017/cbo9780511807435.006

Ali, G. A., Roy, A. G., Turmel, M.-C., & Courchesne, F. (2010). Source-to-stream connectivity assessment through end-member mixing analysis. *Journal of Hydrology*, *392*(3-4), 119-135. https://doi.org/10.1016/j.jhydrol.2010.07.049

Barnett, T. P., Adam, J. C., & Lettenmaier, D. P. (2005). Potential impacts of a warming climate on water availability in snow-dominated regions. *Nature*, *438*(7066), 303-309. https://doi.org/10.1038/nature04141

Barthold, F. K., Tyralla, C., Schneider, K., Vaché, K. B., Frede, H.-G., & Breuer, L. (2011). How many tracers do we need for end member mixing analysis (EMMA)? A sensitivity analysis. *Water Resources Research*, *47*(8). https://doi.org/10.1029/2011wr010604

Barthold, F. K., Wu, J., Vaché, K. B., Schneider, K., Frede, H.-G., & Breuer, L. (2010). Identification of geographic runoff sources in a data sparse region: hydrological processes and the limitations of tracer-based approaches. *Hydrological Processes*, *24*(16), 2313-2327. https://doi.org/10.1002/hyp.7678

Bazemore, D. E., Eshleman, K. N., & Hollenbeck, K., J. (1994). The role of soil water in stormflow generation in a forested headwater catchment: synthesis of natural tracer and hydrometric evidence.

Brooks, P. D., Gelderloos, A., Wolf, M. A., Jamison, L. R., Strong, C., Solomon, D. K., Bowen, G. J., Burian, S., Tai, X., Arens, S., Briefer, L., Kirkham, T., & Stewart, J. (2021). Groundwater-Mediated Memory of Past Climate Controls Water Yield in Snowmelt-Dominated Catchments. *Water Resources Research*, *57*(10). https://doi.org/10.1029/2021wr030605

Butt, R. (2011). *Applied Linear Algebra and Optimization using MATLAB®*. Mercury Learning and Information.

Carling, G. T., Tingey, D. G., Fernandez, D. P., Nelson, S. T., Aanderud, Z. T., Goodsell, T. H., & Chapman, T. R. (2015). Evaluating natural and anthropogenic trace element inputs along an alpine to urban gradient in the Provo River, Utah, USA. *Applied Geochemistry*, *63*, 398-412. https://doi.org/10.1016/j.apgeochem.2015.10.005

Cattell, R. B. (1966). The Scree Test For The Number Of Factors. *Multivariate Behav Res*, *1*(2), 245-276. https://doi.org/10.1207/s15327906mbr0102_10

Checketts, H. N., Carling, G. T., Fernandez, D. P., Nelson, S. T., Rey, K. A., Tingey, D. G., Hale, C. A., Packer, B. N., Cordner, C. P., Dastrup, D. B., & Aanderud, Z. T. (2020). Trace Element Export From the Critical Zone Triggered by Snowmelt Runoff in a Montane Watershed, Provo River, Utah, USA. *Frontiers in Water*, *2*. https://doi.org/10.3389/frwa.2020.578677

Chisola, M. N., van der Laan, M., & Butler, M. J. (2022). Quantifying streamflow sources to improve water allocation management in a catchment undergoing agricultural intensification. *Physics and Chemistry of the Earth, Parts A/B/C*, *128*. https://doi.org/10.1016/j.pce.2022.103227

Christophersen, N. N., C.; Hooper, R. P.; Vogt, R. D.; Anderson, S. . (1990). Modelling streamwater chemistry as a mixture of soilwater end-members - A step towards second-generation acidification models. *Journal of Hydrology*(116), 307-320.

Christopherson, N., & Hooper, R. P. (1992). Multivariate analysis of stream water chemical data: The use of principal components analysis for the end-member mixing problem. *Water Resources Research*, *28*(1), 99-107.

Christopherson, N., Neal, C., Hooper, R. P., Vogt, R. D., & Andersen, S. (1990). Modelling streamwater chemistry as a mixture of soilwater end-members - An application to the Panola Mountain catchment, Georgia U.S.A. *Journal of Hydrology*, *116*, 321-343.

Clark, I. D., & Fritz, P. (1997). *Environmental Isotopes in Hydrogeology*. CRC Press/Lewis Publishers.

Cuoco, E., Viaroli, S., Darrah, T. H., Paolucci, V., Mazza, R., & Tedesco, D. (2021). A geometrical method for quantifying endmembers' fractions in three-component groundwater mixing. *Hydrological Processes*, *35*(11). https://doi.org/10.1002/hyp.14409

Davis, J. C. (2002). *Statistics and Data Analysis in Geology* (3rd ed.). John Wiley & Sons.

Durand, P., & Torres, J. L. J. (1996). Solute transfer in agricultural catchments: the interest and limits of mixing models.

Foks, S. S., Stets, E. G., Singha, K., & Clow, D. W. (2018). Influence of climate on alpine stream chemistry and water sources. *Hydrological Processes*, *32*(13), 1993-2008. https://doi.org/10.1002/hyp.13124

Genereux, D. (1998). Quantifying uncertainty in tracer-based hydrograph separations. *Water Resources Research*, *34*(4), 915-919. https://doi.org/10.1029/98wr00010

Gentle, J. E. (1998). *Numerical linear algebra for applications in statistics*. Springer-Verlag New York, Inc.

Guinn, C. G., Vulava, V. M., Callahan, T. J., Jones, M. L., & Ginn, C. L. (2010). Using water chemistry data to quantify source contribution to stream flow in a coastal plain watershed.

Hale, C. A., Carling, G. T., Nelson, S. T., Fernandez, D. P., Brooks, P. D., Rey, K. A., Tingey, D. G., Packer, B. N., & Aanderud, Z. T. (2022). Strontium isotope dynamics reveal streamflow contributions from shallow flow paths during snowmelt in a montane watershed, Provo River, Utah, USA. *Hydrological Processes*, *36*(1). https://doi.org/10.1002/hyp.14458

Hooper, R. P. (2003). Diagnostic tools for mixing models of stream water chemistry. *Water Resources Research*, *39*(3). https://doi.org/10.1029/2002wr001528

James, A. L., & Roulet, N. T. (2006). Investigating the applicability of end-member mixing analysis (EMMA) across scale: A study of eight small, nested catchments in a temperate forested watershed. *Water Resources Research*, *42*(8). https://doi.org/10.1029/2005wr004419

Joreskog, K. G., Klovan, J. E., & Reyment, R. A. (1976). *Geological Factor Analysis*. Elsevier Scientific Publishing Company.

Liu, F., Williams, M. W., & Caine, N. (2004). Source waters and flow paths in an alpine catchment, Colorado Front Range, United States. *Water Resources Research*, *40*(9). https://doi.org/10.1029/2004wr003076

Lukens, E., Neilson, B. T., Williams, K. H., & Brahney, J. (2022). Evaluation of hydrograph separation techniques with uncertain end-member composition. *Hydrological Processes*, *36*(9). https://doi.org/10.1002/hyp.14693

Montagud, D., Sala, M., & Camarero, L. (2021). Applicability of mixing modelling to determine the contributions to surface flow in high mountain catchments. *Hydrological Sciences Journal*, *66*(16), 2382-2394. https://doi.org/10.1080/02626667.2021.1985723

Munroe, J. S., Attwood, E. C., O'Keefe, S. S., & Quackenbush, P. J. M. (2015). Eolian deposition in the alpine zone of the Uinta Mountains, Utah, USA. *Catena*, *124*, 119-129.

Munroe, J. S., Norris, E. D., Olson, P. M., Ryan, P. C., Tappa, M. J., & Beard, B. L. (2020). Quantifying the contribution of dust to alpine soils in the periglacial zone of the Uinta Mountains, Utah, USA. *Geoderma*, *378*. https://doi.org/10.1016/j.geoderma.2020.114631

Trauth, M. H. (2021). *MATLAB recipes for earth sciences* (5 ed.). Springer Nature Switzerland AG.

Vonk, J. E., Sánchez-García, L., Semiletov, I. P., Dudarev, O. V., Eglinton, T. I., Andersson, A., & Gustafsson, Ö. (2010). Molecular and radiocarbon constraints on sources and degradation of terrestrial organic carbon along the Kolyma paleoriver transect, East Siberian Sea. https://doi.org/10.5194/bgd-7-5191-2010

Wilson, A. M., Williams, M. W., Kayastha, R. B., & Racoviteanu, A. (2016). Use of a hydrologic mixing model to examine the roles of meltwater, precipitation and groundwater in the Langtang River basin, Nepal. *Annals of Glaciology*, *57*(71), 155-168. https://doi.org/10.3189/2016AoG71A067

Xu Fei, E., & Harman, C. J. (2022). A data-driven method for estimating the composition of end-members from stream water chemistry time series. *Hydrology and Earth System Sciences*, *26*(8), 1977-1991. https://doi.org/10.5194/hess-26-1977-2022